

Quantum Algorithms for Stochastic Differential Equations: A Schrödingerisation Approach

Shi Jin^{1,2,3,4}, Nana Liu^{1,2,3,4,5}, Wei Wei¹ *

¹*Institute of Natural Sciences, Shanghai Jiao Tong University, Shanghai 200240, China*

²*School of Mathematical Sciences, Shanghai Jiao Tong University, Shanghai 200240, China*

³*Ministry of Education Key Laboratory in Scientific and Engineering Computing,
Shanghai Jiao Tong University, Shanghai 200240, China*

⁴*Shanghai Artificial Intelligence Laboratory, Shanghai, China*

⁵*University of Michigan-Shanghai Jiao Tong University Joint Institute, Shanghai 200240, China.*

Abstract

Quantum computers are known for their potential to achieve up-to-exponential speedup compared to classical computers for certain problems. To exploit the advantages of quantum computers, we propose quantum algorithms for linear stochastic differential equations, utilizing the Schrödingerisation method for the corresponding approximate equation by treating the noise term as a (discrete-in-time) forcing term. Our algorithms are applicable to stochastic differential equations with both Gaussian noise and α -stable Lévy noise. The gate complexity of our algorithms exhibits an $\mathcal{O}(d \log(Nd))$ dependence on the dimensions d and sample sizes N , where its corresponding classical counterpart requires nearly exponentially larger complexity in scenarios involving large sample sizes. In the Gaussian noise case, we show the strong convergence of first order in the mean square norm for the approximate equations. The algorithms are numerically verified for the Ornstein–Uhlenbeck processes, geometric Brownian motions, and one-dimensional Lévy flights.

1 Introduction

Stochastic differential equations (SDEs) finds applications in various fields including physics, climate modeling, finance and machine learning [32, 42, 33, 45]. Their broad applicability stems from their ability to encapsulate the randomness in nature, providing insights into the dynamics of complex systems with uncertainty. For example, the stochastic Langevin equation and its variants are widely applied in physics and machine learning, including generative AI [11, 13, 21, 42]. Another important application of SDEs is in Monte Carlo simulations, where SDEs are used to model and simulate random processes over time.

For many applications, it becomes interesting to develop quantum algorithms to leverage the potential advantage offered by quantum computers. Quantum computers, which are different from their classical counterparts, use qubits instead of bits. Some of the quantum algorithms have already proved to have quantum advantages over their classical counterparts in, for example, searching (Grover’s algorithm) [17], cryptography (Shor’s algorithm) [41], sampling (Boson sampling) [1], solving linear algebraic equations (the HHL algorithm) [9, 18] and etc. Quantum algorithms also have applications in computational finance, which is also closely related to stochastic differential equations [16, 34, 40].

Although classical schemes for SDE, such as the Euler-Maruyama scheme, have been proposed for decades and are widely used in various areas, the quantum algorithms for SDE are underdeveloped.

The motivation for designing quantum algorithms for SDEs arises from the fact that, while simulating a single sample path incurs only a manageable computational cost, achieving a target precision ϵ with the Monte Carlo method requires at least $\mathcal{O}(1/\epsilon^2)$ simulations, leading to substantial computational expense [4]. Several quantum algorithms have been proposed for SDEs and Monte Carlo simulations. Reference [34] develops a quantum-classical hybrid algorithm based on variational quantum simulation. It discretizes the SDE into a trinomial tree model and computes the nodes of the tree by time-evolution of a quantum state.

*weiw_sjtu@sjtu.edu.cn

The nodes of the tree of each level represent the distribution of the SDE at each time step. However, the tree model itself suffers from insufficient accuracy. Reference [38] guarantees the near-quadratic speedup of quantum computers in the sampling process of Monte Carlo methods. Based on this, reference [4] develops quantum algorithms for multi-level Monte Carlo simulation with simulation of SDEs. However, it is developed based on oracles for the expectation of SDEs, and does not offer a concrete quantum algorithm. Reference [12] uses the relationship between open quantum systems, SDEs, and Hamiltonian simulations to develop high order quantum algorithms for the open quantum system. Thus, quantum algorithms for SDEs that both match the accuracy of classical schemes and offers greater efficiency, are of significant interest.

Recently, a Schrödingerisation approach [29, 27] has been proposed to solve general linear ordinary and partial differential equations via Hamiltonian simulation, which can also be implemented in quantum circuits [19, 28] and applicable to a wide variety of differential equations [20, 25, 24, 26, 30]. The method of Schrödingerisation involves the incorporation of an auxiliary variable to transform a linear differential equation into an equation analogous to the Schrödinger equation, with unitary evolution process, in one higher dimension. Subsequently, the transformed equation lends itself to implementation on quantum computers through Hamiltonian simulation. The desired result is recovered from the Schrödingerised equation on a properly chosen interval of the auxiliary variable. This method maintains the major structure of the original classical differential equations, thus, consequently, one can develop quantum algorithms that retain the convergence rate of classical schemes while leveraging the benefits of quantum computing.

In this paper, we propose a general quantum algorithm to simulate the solutions of linear SDEs, including SDEs with additive noise and multiplicative noise. The main idea is to treat the noise term as a discrete-in-time forcing term and then uses the Schrödingerisation method for inhomogeneous differential equations [24]. While most quantum algorithms focus on SDEs with Gaussian noise, our approach is applicable to SDEs driven by stable Lévy processes, which is a more general type of noise. We design the quantum algorithms for the approximate equation through the Schrödingerisation method, which approximates the corresponding SDEs under mean square norm in the Gaussian noise case. We also discuss the important issue of the choice of the recovery interval and its influence on the precision of the final result. Theoretically, for both the additive and multiplicative Gaussian noise cases, we prove the strong convergence of first order for the approximate solution. The quantum advantage of our algorithm is exhibited by its gate complexity of $\mathcal{O}(d \log(Nd))$ dependence on the dimensions d and the sample size N , which is a nearly exponential speed-up compared to its classical counterparts. We illustrate the validation of the algorithms to the Ornstein–Uhlenbeck processes, geometric Brownian motions and one-dimensional Lévy flights by numerical experiments.

This paper is organized as follows: Section 2 introduces the approximate equations for both SDEs with additive noise and multiplicative noise. By the Schrödingerisation method, we provide the technical details of the quantum algorithms for SDEs. We give the gate complexity of our quantum algorithm in subsection 2.4 and provide a complexity analysis which demonstrates the quantum advantage for dimensions and sample sizes. In Section 3, we show the correctness of our method by numerical experiments for a one dimensional Ornstein–Uhlenbeck process, a one dimensional geometric Brownian motion and a one dimensional Lévy flight. In Section 4, we show the convergence rate of the approximate equations in the mean square norm. Together with the error of the recovery part, we give the overall error of our algorithms. We summarize our method and discuss further applications in Section 5.

2 Quantum simulation for SDEs

In this section, we will introduce the quantum simulation scheme for linear SDE with Gaussian noise. The scheme is based on the combination of the Euler-Maruyama scheme and the Schrödingerisation technique [29, 27].

2.1 Linear SDE with additive Gaussian noise

Given a probability space $(\Omega, \mathcal{F}, \mathbb{P})$, we consider the following d -dimensional SDE:

$$dX_t = AX_t dt + B dW_t, \quad X_0 = x_0, \quad 0 \leq t \leq T. \quad (1)$$

Here, W_t is the d -dimensional standard Brownian motion. A and B are $d \times d$ matrices.

The Euler-Maruyama scheme for equation (1) is described as follows.

Let $t_k = kT/N_T$, $\Delta t = T/N_T$, and $\{\widehat{X}(t_k)\}_{0 \leq k \leq N}$ be the numerical solution to (1):

$$\widehat{X}(t_{k+1}) = \widehat{X}(t_k) + A\widehat{X}(t_k)\Delta t + B\Delta W_k, \quad \widehat{X}(t_0) = x_0 \text{ and } k = 0, 1, \dots, N_T - 1 \quad (2)$$

where $\Delta W_k = W_{t_{k+1}} - W_{t_k}$ is a Gaussian random variable with mean 0 and covariance matrix $\Delta t I$.

We first replace the discrete time in the Euler-Maruyama method with a continuous time variable, so it becomes an ordinary differential equation for each time interval. More precisely, for the temporal mesh $\{t_k = k\Delta t : \Delta t = T/N_T, k = 0, 1, \dots, N_T\}$, we aim to calculate the solution of the following ordinary differential equation in the k -th iteration:

$$\begin{cases} \frac{d}{dt} \widetilde{X}(t) = A\widetilde{X}(t) + \frac{B\Delta W_k}{\Delta t}, & t_k < t \leq t_{k+1}, \quad k \geq 1, \\ \text{with } \widetilde{X}(t_k) \text{ calculated in the } (k-1)\text{-th iteration.} \end{cases} \quad (3)$$

Here $\widetilde{X}(t_0) = x_0$ and $\Delta W_k = W_{t_{k+1}} - W_{t_k}$ which can be simulated by a group of independent d -dimensional standard Gaussian random variables $\{\boldsymbol{\xi}_k : \boldsymbol{\xi}_k \sim N(0, \mathbf{I})\}$:

$$\Delta W_k \stackrel{d}{=} \sqrt{\Delta t} \boldsymbol{\xi}_k.$$

Now we can implement the Schrödingerisation procedure [27] to (3). Take

$$\widetilde{A}_k = \begin{pmatrix} A & B\Delta W_k/\sqrt{\Delta t} \\ \mathbf{0}^\top & 0 \end{pmatrix}, \quad \widetilde{Y} = \begin{pmatrix} \widetilde{X}(t) \\ 1/\sqrt{\Delta t} \end{pmatrix},$$

then equation (3) becomes,

$$\begin{cases} \frac{d}{dt} \widetilde{Y}(t) = \widetilde{A}_k \widetilde{Y}(t), & t_k \leq t \leq t_{k+1}, \\ \widetilde{Y}(0) = (x_0, 1/\sqrt{\Delta t})^\top. \end{cases} \quad (4)$$

For every \widetilde{A}_k , we decompose it into a Hermitian matrix $H_{1,k}$ and an anti-Hermitian matrix $iH_{2,k}$.

$$\widetilde{A}_k = H_{1,k} + iH_{2,k},$$

where

$$H_{1,k} = \frac{\widetilde{A}_k + \widetilde{A}_k^\dagger}{2} = H_{1,k}^\dagger, \quad H_{2,k} = \frac{\widetilde{A}_k - \widetilde{A}_k^\dagger}{2i} = H_{2,k}^\dagger.$$

Apply the warped phase transformation to \widetilde{Y} , that is taking $\mathbf{v}(t, p) = e^{-p\widetilde{Y}(t)}$ for $p > 0$. Then, $\mathbf{v}(t, p)$ satisfies the $(d+1)$ -dimensional equation

$$\begin{cases} \frac{d}{dt} \mathbf{v}(t, p) = -H_{1,k} \partial_p \mathbf{v}(t, p) + iH_{2,k} \mathbf{v}(t, p), & t_k < t \leq t_{k+1}, \\ \mathbf{v}(0, p) = e^{-|p|} \widetilde{Y}(0), & p \in (-\infty, \infty). \end{cases} \quad (5)$$

By taking the Fourier transform of $\mathbf{v}(t, p)$ with respect to p and denoting it as $w(t, \eta)$, we obtain

$$\begin{cases} \frac{d}{dt} w(t, \eta) = -i\eta H_{1,k} w(t, \eta) + iH_{2,k} w(t, \eta), & t_k < t \leq t_{k+1}, \\ w(0, \eta) = \frac{1}{\pi(1 + \eta^2)} \widetilde{Y}(0). \end{cases} \quad (6)$$

Here we have derived an equation (6) analogous to the Schrödinger equation.

If all eigenvalues of $H_{1,k}$ are negative, the solution $\widetilde{Y}(t)$ can be restored by the integration:

$$\widetilde{Y}(t) = \int_0^\infty \mathbf{v}(t, p) dp.$$

If $H_{1,k}$ contains some positive eigenvalues, which will be the case with the noise term, then $\tilde{Y}(t)$ can still be restored through the normalized integration formula:

$$\tilde{Y}(t) = \frac{\int_{p^*}^{p^{**}} \mathbf{v}(t, p) dp}{\int_{p^*}^{p^{**}} e^{-p} dp}, \quad (7)$$

where $p^{**} > p^* > \lambda_{\max}^+(H_{1,k})T$, with $\lambda_{\max}^+(H_{1,k})$ being the largest positive eigenvalues of $H_{1,k}$ for $t \in (0, T)$ [24].

In Section 4, we will show in Proposition 4.7 that the mean square norm between \tilde{X} and X satisfies

$$\|\tilde{X}(T) - X(T)\|_{L^2} \lesssim \Delta t.$$

Remark 2.1. Equation (6) can be seen as a piecewise constant time-dependent Schrödinger equation with Hamiltonian $\tilde{H}(t)$ defined by

$$\tilde{H}(t) = \sum_{k=0}^{N_T-1} (\eta H_{1,k} - H_{2,k}) \mathbb{1}_{(t_k, t_{k+1}]}(t),$$

where $H_{1,k}$ and $H_{2,k}$ are linear Hermitian random matrix. The random matrix $H_{1,k}$ and $H_{2,k}$ have the following explicit expression:

$$H_{1,k} = \begin{pmatrix} \frac{1}{2}(A + A^\dagger) & \frac{1}{2}B\Delta W_k/\sqrt{\Delta t} \\ \frac{1}{2}(\Delta W_k^\top/\sqrt{\Delta t})B^\dagger & 0 \end{pmatrix}, \quad H_{2,k} = \begin{pmatrix} \frac{1}{2i}(A - A^\dagger) & -\frac{i}{2}B\Delta W_k/\sqrt{\Delta t} \\ \frac{i}{2}(\Delta W_k^\top/\sqrt{\Delta t})B^\dagger & 0 \end{pmatrix}.$$

Remark 2.2. The Schrödingerisation procedure can also be applied to linear SDE driven by α -stable Lévy processes with $1 < \alpha < 2$. Specifically, consider a d -dimensional linear SDE driven by isotropic α -stable Lévy processes:

$$dX_t = AX_t dt + BdL_t^\alpha, \quad X_0 = x_0, \quad 0 \leq t \leq T, \quad (8)$$

where L_t^α is a d -dimensional isotropic α -stable Lévy process with $1 < \alpha < 2$ and it satisfies $L_t^\alpha \stackrel{d}{=} t^{\frac{1}{\alpha}} L_1$. Then we can proceed with the approximate equation

$$\begin{cases} \frac{d}{dt} \tilde{X}(t) = A\tilde{X}(t) + \frac{B\Delta L_k^\alpha}{\Delta t}, & t_k < t \leq t_{k+1}, \quad k \geq 1, \\ \text{with } \tilde{X}(t_k) \text{ calculated in the } (k-1)\text{-th iteration.} \end{cases} \quad (9)$$

Here $X(t_0) = x_0$ and $\Delta L_k^\alpha = L_{t_{k+1}}^\alpha - L_{t_k}^\alpha \stackrel{d}{=} \Delta t^{\frac{1}{\alpha}} L_1$ are independent with identical stable distribution. Take random variables $\xi_k \stackrel{d}{=} L_1$. We can proceed with the above arguments for SDE with additive Gaussian noise by replacing the matrix A_k with

$$\tilde{A}_k = \begin{pmatrix} A & B\Delta t^{\frac{1}{\alpha}} \xi_k \\ 0 & 0 \end{pmatrix}, \quad \tilde{Y}(t) = \begin{pmatrix} \tilde{X}(t) \\ \frac{1}{\Delta t} \end{pmatrix}.$$

Here, the one stage approximation of the approximate equation (9) is the same as the Euler-Maruyama scheme for the SDE (8). And the Euler-Maruyama scheme itself is proven to admit strong rate of convergence in this case, see [35]. For $0 < \alpha < 1$, the moments of the α -stable Lévy process do not exist, hence we do not consider this case in this paper. In Section 3, we present a numerical example of a one dimensional Lévy flight.

2.2 Linear SDE with multiplicative Gaussian noise

We consider the following SDE:

$$dX(t) = AX(t)dt + \sum_{l=1}^m B^{(l)}X(t)dW_t^{(l)}, \quad X_0 = x_0. \quad (10)$$

Here, $W_t = (W_t^{(1)}, \dots, W_t^{(m)})$ is a m -dimensional standard Brownian motion. $\{A, B^{(1)}, \dots, B^{(m)}\}$ are $d \times d$ matrices.

We introduce the following approximate equation for the Schrödingerisation approach. For $t_k = kT/N_T$, we aim to compute the following ordinary differential equation,

$$\begin{cases} \frac{d\tilde{X}(t)}{dt} = \tilde{A}_k \tilde{X}(t), & \tilde{X}(0) = x_0 \text{ and } t_k \leq t \leq t_{k+1} \\ \tilde{A}_k = A - \frac{1}{2} \sum_{l=1}^m (B^{(l)})^2 + \sum_{l=1}^m B^{(l)} \frac{\Delta W_k^{(l)}}{\Delta t}, \end{cases} \quad (11)$$

where $\Delta W_k^{(l)} = W_{t_{k+1}}^{(l)} - W_{t_k}^{(l)}$ is a standard scalar Gaussian random variable. The summation $-\frac{1}{2} \sum_{l=1}^m (B^{(l)})^2$ is from the correction term of the Ito's formula.

Similarly as the additive noise case (4), we decompose \tilde{A}_k into a Hermitian matrix $H_{1,k}$ and an anti-Hermite matrix $iH_{2,k}$.

$$\tilde{A}_k = H_{1,k} + iH_{2,k},$$

where

$$H_{1,k} = \frac{\tilde{A}_k + \tilde{A}_k^\dagger}{2} = H_{1,k}^\dagger, \quad H_{2,k} = \frac{\tilde{A}_k - \tilde{A}_k^\dagger}{2i} = H_{2,k}^\dagger.$$

Through the warped phase transformation to \tilde{X} to get $\mathbf{v}(t, p)$ and the Fourier transformation on the auxiliary variable p to derive $w(t, \eta)$, we arrive at the equation analogous to the Schrödinger equation

$$\begin{cases} \frac{d}{dt} w(t, \eta) = -i\eta H_{1,k} w(t, \eta) + iH_{2,k} w(t, \eta), & t_k < t \leq t_{k+1}, \\ w(0, \eta) = \frac{1}{\pi(1+\eta^2)} \tilde{X}(0). \end{cases} \quad (12)$$

Then we can follow exactly the same steps as in the additive noise case to solve equation (12) by the Hamiltonian simulation and recover the solution through the normalized integration formula (7).

Different from the additive noise case, equation (11) is already a homogeneous system so we do not need to expand \tilde{X} into a $(d+1)$ -dimensional vector Y .

In Section 4, we will show in Proposition 4.8 the mean square norm between \tilde{X} and X satisfies

$$\|\tilde{X}(T) - X(T)\|_2 \lesssim \Delta t.$$

Remark 2.3. If we assume the matrices $\{B^{(1)}, \dots, B^{(m)}\}$ commute, that is

$$B^{(k)} B^{(l)} = B^{(l)} B^{(k)},$$

by the definition of the matrix exponential, we get the one stage approximation

$$\begin{aligned} \tilde{X}(t_{k+1}) &= \tilde{X}(t_k) + \tilde{A}_k \tilde{X}(t_k) \Delta t + \frac{1}{2} \sum_{l=1}^m \sum_{j=1}^m B^{(l)} B^{(j)} \tilde{X}(t_k) \Delta W_k^{(l)} \Delta W_k^{(j)} + \mathcal{O}(\Delta t \Delta W) \\ &= \tilde{X}(t_k) + A \tilde{X}(t_k) \Delta t + \sum_{l=1}^m B^{(l)} \tilde{X}(t_k) \Delta W_k^{(l)} + \frac{1}{2} \sum_{l=1}^m (B^{(l)})^2 \tilde{X}(t_k) ((\Delta W_k^{(l)})^2 - \Delta t) \\ &\quad + \frac{1}{2} \sum_{\substack{l,j=1 \\ l \neq j}}^m B^{(l)} B^{(j)} \tilde{X}(t_k) \Delta W_k^{(l)} \Delta W_k^{(j)} + \mathcal{O}(\Delta t \Delta W), \end{aligned}$$

which is the Milstein scheme (see, for example, [31, Section 10.3]) for SDE (10).

If we further assume that matrices $\{A, B^{(1)}, \dots, B^{(m)}\}$ commute, the analytical solution to (10) is ([31, Section 4.8]),

$$X(t) = x_0 \exp \left[\left(A - \frac{1}{2} \sum_{l=1}^m (B^{(l)})^2 \right) t + \sum_{l=1}^m B^{(l)} W_t^{(l)} \right]. \quad (13)$$

In this case, it is clear that

$$\tilde{X}(t_k) = x_0 \exp \left[\left(A - \frac{1}{2} \sum_{l=1}^m (B^{(l)})^2 \right) t_k + \sum_{l=1}^m B^{(l)} \sum_{j=0}^k \Delta W_j^{(l)} \right],$$

which is exactly the sample path of (13).

2.3 Discrete numerical form

In this section, we will numerically solve the linear differential equation arose in (4) and (11), which takes the form

$$\frac{dZ(t)}{dt} = \tilde{A}_k Z(t), \quad Z(0) = z_0 \text{ and } t_k \leq t \leq t_{k+1}.$$

Here $Z \in \mathbb{R}^{\tilde{d}}$, where $\tilde{d} = d + 1$ for the additive noise case and $\tilde{d} = d$ for the multiplicative noise case.

By the warped phase transformation, we arrive to solve the linear equation

$$\begin{cases} \frac{d}{dt} \mathbf{v}(t, p) = -H_{1,k} \partial_p \mathbf{v}(t, p) + iH_{2,k} \mathbf{v}(t, p), & t_k < t \leq t_{k+1}, \\ \mathbf{v}(0, p) = e^{-|p|} z_0, & p \in (-\infty, \infty). \end{cases} \quad (14)$$

Next, we will numerically solve equation (14) by the discrete Fourier transform on a sufficiently large interval $[-L, L]$ so that $e^{-L} \approx 0$. We adopt the symbols in [27] and refer to [27, Sec.II.A.2] for more details.

Let $\Delta p = L/N$. For $p_j = -L + (j-1)\Delta p$, denote

$$\mathbf{w}(t) := [\mathbf{w}_1(t); \mathbf{w}_2(t); \cdots; \mathbf{w}_{2N}(t)] = \sum_{j=1}^{2N} \sum_{h=1}^{\tilde{d}} v_h(t, p_j) |j\rangle \otimes |h\rangle, \quad \mathbf{w}_j(t) = \sum_{h=1}^{\tilde{d}} v_h(t, p_j) |h\rangle.$$

Here $v_h |h\rangle$ is the \tilde{d} -dimensional vector with the h -th entry being the h -th entry v_h of \mathbf{v} and the other entries being zero. $|j\rangle$ is the j -th computational basis corresponding to the j -th point in the mesh of the variable p . The symbol “;” indicates the straightening of $\{\mathbf{w}(t, p_k)\}_{k \geq 0}$ into a column vector. Let $\tilde{\mathbf{w}}$ be the spectral approximation of \mathbf{w} with respect to p , which means

$$\mathbf{w}(t) \approx \tilde{\mathbf{w}}(t) = (\Phi \otimes \mathbf{I}) \tilde{\mathbf{c}}(t).$$

Here,

$$\begin{aligned} \tilde{\mathbf{w}}(t) &:= [\tilde{\mathbf{w}}_1(t); \tilde{\mathbf{w}}_2(t); \cdots; \tilde{\mathbf{w}}_{2N}(t)] = \sum_{j=1}^{2N} \sum_{h=1}^{\tilde{d}} \tilde{w}_h(t, p_j) |j\rangle \otimes |h\rangle, & \tilde{\mathbf{w}}_j(t) &= \sum_{h=1}^{\tilde{d}} \tilde{w}_h(t, p_j) |h\rangle, \\ \tilde{\mathbf{c}}(t) &:= [\mathbf{c}_1(t); \mathbf{c}_2(t); \cdots; \mathbf{c}_{2N}(t)] = \sum_{l=1}^{2N} \sum_{h=1}^{\tilde{d}} c_l^{(h)}(t) |l\rangle \otimes |h\rangle, & \mathbf{c}_l(t) &= \sum_{h=1}^{\tilde{d}} c_l^{(h)}(t) |h\rangle. \end{aligned}$$

and

$$\Phi |l\rangle = \sum_{j=1}^{2N} e^{i\mu_l(p_j+L)} |j\rangle, \quad \tilde{w}_h(t, p_j) = \sum_{l=1}^{2N} c_l^{(h)}(t) e^{i\mu_l(p_j+L)}, \quad \mu_l = \frac{\pi(l-N-1)}{L}.$$

It is clear that Φ^{-1} is the discrete Fourier transform on variable p . Then $\tilde{\mathbf{w}}$ satisfies

$$\partial_t \tilde{\mathbf{w}}(t) = \sum_{k=0}^{N_T-1} -i(P_\mu \otimes H_{1,k} - \mathbf{I} \otimes H_{2,k}) \mathbb{1}_{(t_k, t_{k+1}]}(t) \tilde{\mathbf{w}}(t). \quad (15)$$

Here $P_\mu = -i\partial_p$ is the momentum operator and on the computational basis $\{|j\rangle\}_{1 \leq j \leq 2N}$, it satisfies

$$P_\mu \Phi |l\rangle = \sum_{j=1}^{2N} \mu_l e^{i\mu_l(p_j+L)} |j\rangle.$$

A direct computation shows that $D_{\boldsymbol{\mu}} = \Phi^{-1}P_{\boldsymbol{\mu}}\Phi$ with $D_{\boldsymbol{\mu}} = \text{diag}(\mu_1, \mu_2, \dots, \mu_{2N})$, $\mu_l = \pi(l - N - 1)/L$, then we have

$$\partial_t \tilde{\mathbf{c}}(t) = \sum_{k=0}^{N_T-1} -i(D_{\boldsymbol{\mu}} \otimes H_{1,k} - \mathbf{I} \otimes H_{2,k}) \mathbb{1}_{(t_k, t_{k+1}]}(t) \tilde{\mathbf{c}}(t),$$

which is a system of linear ordinary differential equations. It can be rewritten as

$$\partial_t \tilde{\mathbf{c}}(t) = \sum_{k=0}^{N_T-1} -i(\tilde{H}_{1,k} - \tilde{H}_{2,k}) \mathbb{1}_{(t_k, t_{k+1}]}(t) \tilde{\mathbf{c}}(t), \quad (16)$$

with

$$\tilde{H}_{1,k} = \begin{pmatrix} \mu_1 H_{1,k} & & & \\ & \mu_2 H_{1,k} & & \\ & & \ddots & \\ & & & \mu_{2N} H_{1,k} \end{pmatrix}, \quad \tilde{H}_{2,k} = \begin{pmatrix} H_{2,k} & & & \\ & H_{2,k} & & \\ & & \ddots & \\ & & & H_{2,k} \end{pmatrix}. \quad (17)$$

Denote \mathcal{F}^{-1} as the discrete Fourier transform on variable p ,

$$\mathcal{F}|l\rangle = \frac{1}{\sqrt{2N}} \sum_{j=1}^{2N} e^{i\pi \frac{lj}{N}} |j\rangle, \quad \mathcal{F}^{-1}|j\rangle = \frac{1}{\sqrt{2N}} \sum_{l=1}^{2N} e^{-i\pi \frac{jl}{N}} |l\rangle.$$

Then $\Phi = \sqrt{2N}\mathcal{F}$. Let

$$\tilde{\mathbf{c}}(0) = \frac{1}{\sqrt{2N}} (\mathcal{F}^{-1} \otimes \mathbf{I}) \mathbf{w}(0). \quad (18)$$

Then, we obtain $\tilde{\mathbf{w}}$ by

$$\tilde{\mathbf{w}}(t_k) = \sqrt{2N} (\mathcal{F} \otimes \mathbf{I}) \tilde{\mathbf{c}}(t_k). \quad (19)$$

Furthermore, we can also derive the discrete Fourier approximation $\tilde{\mathbf{w}}^c$ of \mathbf{v} with $\tilde{\mathbf{c}}$:

$$\tilde{\mathbf{w}}^c(t_k, p) = [\tilde{w}_1(t_k, p), \dots, \tilde{w}_d(t_k, p)], \quad \tilde{w}_h(t_k, p) = \sum_{l=1}^{2N} c_l^{(h)}(t) e^{i\mu_l(p+L)}.$$

The numerical approximation of \tilde{X} , denoted by $\tilde{X}^{\tilde{\mathbf{w}}}$, is recovered by the *normalized integration method*

$$\tilde{X}^{\tilde{\mathbf{w}}}(t_k) = \frac{\sum_{p_j \in U_p} \tilde{\mathbf{w}}^c(t_k, p_j) \Delta p}{\sum_{p_j \in U_p} e^{-p_j} \Delta p} \quad (20)$$

where $U_p = [p^*, p^{**}]$.

Remark 2.4. In quantum computers, we can directly obtain $\{\mathbf{c}(t_k)\}$ by Hamiltonian simulation. Note that equation (16) is the system with piecewise constant Hamiltonian and thus we can simply apply schemes for time-independent Hamiltonian simulation multiple times in this case. General time-dependent Hamiltonian simulation algorithms are also applicable here, for example, the Trotterization based methods [2, 3, 44] and a newly proposed method by [8] which transfers the non-autonomous system, that is the time-dependent Hamiltonian system, into an autonomous system in one-higher dimension.

For a verification in classical computers, we use the second order i-stable Runge-Kutta method [5] to solve equation (16) on the temporal mesh $\{t_k = k\Delta t : \Delta t = T/N_T, k = 0, 1, \dots, N_T\}$. It means

$$\begin{aligned} \tilde{\mathbf{c}}(t_{k+1}) &= \tilde{\mathbf{c}}(t_k) + \Delta t K_3, \\ K_1 &= F_k \tilde{\mathbf{c}}(t_k), \quad K_2 = F_k(\tilde{\mathbf{c}}(t_k) + \Delta t K_1/3), \quad K_3 = F_k(\tilde{\mathbf{c}}(t_k) + \Delta t K_2/2), \\ F_k &= -i\tilde{H}_{1,k} + i\tilde{H}_{2,k}, \quad k = 0, 1, \dots, N_T - 1. \end{aligned}$$

An i-stable is a scheme whose stability region contains part of the imaginary axis [5]. Such a property is important since the spectral of the Schrödingerized differential operator are purely imaginary, thus a scheme like forward Euler method will be unstable.

Let $\tilde{H}_1(t) = \sum_{k=0}^{N_T-1} H_{1,k} \mathbb{1}_{(t_k, t_{k+1}]}(t)$, $\lambda_{\max}^-(\tilde{H}_1) = |\min_{t \in [0, T]} \{\lambda(\tilde{H}_1(t)), 0\}|$ and $I = [-L, L]$. In Proposition 4.5, we will show the recovered solution $\tilde{X}^{\tilde{\mathbf{w}}}(t_k)$ satisfy the following estimate,

$$\|\tilde{X}^{\tilde{\mathbf{w}}}(t_k) - \tilde{X}(t_k)\| \lesssim (\Delta p^{\frac{3}{2}} + \sqrt{|\lambda_{\max}^-(\tilde{H}_1)|^2 t_k e^{\lambda_{\max}^-(\tilde{H}_1) - L}}) \|\tilde{Y}(0)\|.$$

2.4 Complexity

For the d -dimensional SDE (1), we will need $d \times (2L)/\Delta p$ grid points for solving the approximate SDE (3). So the number of qubits n that is needed for registers is

$$n \sim \log(1/\Delta p) + \log(d).$$

Given a matrix or vector H , let $\|H\|_{\max}$ denote the largest entry of H in absolute value and $s(H)$ denote the sparsity of H which is the number of nonzero entries of H in every column and row. Denote $\tilde{H}_k = \tilde{H}_{1,k} - \tilde{H}_{2,k}$. The following proposition is from [37, Theorem 3] and it gives the complexity for implementing Hamiltonian simulation.

Proposition 2.5. *A d -sparse Hamiltonian \hat{H} on n qubits with matrix elements specified to τ_b bits of precision can be simulated for time interval t , error ϵ , and success probability at least $1 - 2\epsilon$ with $\mathcal{O}(td\|\hat{H}\|_{\max} + \log(1/\epsilon)/\log\log(1/\epsilon))$ queries and a factor $\mathcal{O}(n + \tau_b \text{polylog}(\tau_b))$ additional quantum gates.*

Hereafter, we assume the precision τ and error ϵ are fixed. The following theorem gives the gate complexity of the Schrödingerisation approach.

Theorem 2.6. *For the d -dimensional SDE with additive Gaussian noise (1), the Schrödingerisation procedure to obtain $\tilde{X}(T)$ of equation (15) has gate complexity*

$$N_{\text{Gate,Schr}} = \mathcal{O}\left(\frac{Td}{\Delta p}\left(\log\left(\frac{1}{\Delta p}\right) + \log(d)\right)\left(\|A\|_{\max} + |\Delta W|_{\max}/\sqrt{\Delta t}\right)\right),$$

where $|\Delta W|_{\max} := \max_{1 \leq k \leq N_T} \|\Delta W_k\|_{\max}$.

Proof. The procedure of the Schrödingerisation approach can be realized as follows:

$$\tilde{\mathbf{w}}(t_0, \cdot) \xrightarrow{F_p^{-1}} \mathbf{c}(t_0) \xrightarrow{e^{-i\tilde{H}_1 \Delta t}} \mathbf{c}(t_1) \cdots \xrightarrow{e^{-i\tilde{H}_k \Delta t}} \mathbf{c}(t_k) \cdots \xrightarrow{e^{-i\tilde{H}_{N_T} \Delta t}} \mathbf{c}(T) \xrightarrow{F_p} \tilde{\mathbf{w}}(T, \cdot) \quad (21)$$

where $\tilde{H}_k = \tilde{H}_{1,k} - \tilde{H}_{2,k}$ and $F_p = \Phi$ is the discrete Fourier transform. The Hamiltonian simulation using the Hamiltonian \tilde{H}_k is employed in the intermediate steps. It is clear from (18) that F_p can be realized based on quantum Fast Fourier transform (see, for example, [41]). So, the Schrödingerisation procedure can be realized by quantum Fast Fourier transform and Hamiltonian simulation. According to Proposition 2.5, we need to compute the sparsity $s(\tilde{H}_k)$ and $\|\tilde{H}_k\|_{\max}$.

For $s(\tilde{H}_k)$,

$$\begin{aligned} s(\tilde{H}_k) &= s(\tilde{H}_{1,k} - \tilde{H}_{2,k}) = s(D_{\boldsymbol{\mu}} \otimes H_{1,k} - \mathbf{I} \otimes H_{2,k}) \\ &\leq \max_{1 \leq l \leq 2N} s(\mu_l H_{1,k} - H_{2,k}) \leq d + 1. \end{aligned}$$

For $\|\tilde{H}_k\|_{\max}$,

$$\begin{aligned} \|\tilde{H}_k\|_{\max} &= \|D_{\boldsymbol{\mu}} \otimes H_{1,k} - \mathbf{I} \otimes H_{2,k}\|_{\max} \\ &\leq \max_{1 \leq l \leq 2N} \|\mu_l H_{1,k}\|_{\max} + \|H_{2,k}\|_{\max} \\ &\leq (\pi/\Delta p + 1)(\|A\|_{\max} + |\Delta W|_{\max}/\sqrt{\Delta t}). \end{aligned}$$

Here $|\Delta W|_{\max} := \max_{1 \leq k \leq N_T} |\Delta W_k|$.

Let n_p denote the number of qubits that is needed for the p -variable. It known that the one-dimensional quantum Fourier transform on n_p qubits can be implemented using $\mathcal{O}(n_p \log n_p)$ gates [39]. By proposition 2.5, for fixed m bits of precision and error ϵ , the overall gate complexity to obtain $\tilde{\mathbf{w}}(T, \cdot)$ is

$$\begin{aligned} N_{\text{gates,Schr}} &= \mathcal{O}(n_p \log n_p) + N_T \mathcal{O}\left(n(\Delta t \max_{1 \leq k \leq 2N} \{s(\tilde{H}_k)\|\tilde{H}_k\|_{\max}\})\right) \\ &\leq \mathcal{O}(n_p \log n_p) + \mathcal{O}(Td(\log(1/\Delta p) + \log(d))(\|A\|_{\max} + |\Delta W|_{\max}/\sqrt{\Delta t})/\Delta p). \end{aligned}$$

As $n_p \sim \log(1/\Delta p)$, we have

$$N_{\text{gates,Schr}} = \mathcal{O} \left(\frac{Td}{\Delta p} \left(\log\left(\frac{1}{\Delta p}\right) + \log(d) \right) \left(\|A\|_{\max} + |\Delta W|_{\max}/\sqrt{\Delta t} \right) \right). \quad (22)$$

With the state $\tilde{w}(T, \cdot)$, to recover $\tilde{X}(T)$, we can directly apply the projection measurement $\sum_{j^*}^{j^{**}} |j\rangle\langle j|$ where $p = j\Delta p$ and the state $\tilde{X}(T)/\|\tilde{X}(t)\|$ can be recovered with probability $O(\|\tilde{X}(T)\|^2/\|\tilde{X}(0)\|^2)$ [23, 29]. So, the overall gate complexity to derive $\tilde{X}(T)$ is the same as (22). \square

With similar arguments, we can derive the gate complexity for the SDE with multiplicative noise.

Corollary 2.7. *For the d -dimensional SDE with multiplicative Gaussian noise (10), the Schrödingerisation procedure to obtain $\tilde{X}(T)$ has gate complexity*

$$N_{\text{gates,Schr}} = \mathcal{O} \left(\frac{Td}{\Delta p} \left(\log\left(\frac{1}{\Delta p}\right) + \log(d) \right) \left(\|A\|_{\max} + m\|B\|_{\max}^2 + \frac{m\|B\|_{\max}|\Delta W|_{\max}}{\Delta t} \right) \right),$$

where $\Delta t = T/N_T$.

Proof. Similar as Theorem 2.6, we only need to compute the sparsity $s(\tilde{H}_k)$ and $\|\tilde{H}_k\|_{\max}$.

As \tilde{A}_k is a d -dimensional matrix and

$$\begin{aligned} \|\tilde{A}_k\|_{\max} &= \left\| A - \frac{1}{2} \sum_{l=1}^m (B^{(l)})^2 + \sum_{l=1}^m B^{(l)} \frac{\Delta W_k^{(l)}}{\Delta t} \right\|_{\max} \\ &\lesssim \|A\|_{\max} + m\|B\|_{\max}^2 + \frac{m\|B\|_{\max}|\Delta W|_{\max}}{\Delta t}. \end{aligned}$$

For $s(\tilde{H}_k)$,

$$\begin{aligned} s(\tilde{H}_k) &= s(\tilde{H}_{1,k} - \tilde{H}_{2,k}) = s(D_{\mu} \otimes H_{1,k} - \mathbf{I} \otimes H_{2,k}) \\ &\leq \max_{1 \leq l \leq 2N} s(\mu_l H_{1,k} - H_{2,k}) \leq d. \end{aligned}$$

For $\|\tilde{H}_k\|_{\max}$,

$$\begin{aligned} \|\tilde{H}_k\|_{\max} &= \|D_{\mu} \otimes H_{1,k} - \mathbf{I} \otimes H_{2,k}\|_{\max} \\ &\leq \max_{1 \leq l \leq 2N} \|\mu_l H_{1,k}\|_{\max} + \|H_{2,k}\|_{\max} \\ &\leq (\pi/\Delta p + 1) (\|A\|_{\max} + m\|B\|_{\max}^2 + \frac{m\|B\|_{\max}|\Delta W|_{\max}}{\Delta t}). \end{aligned}$$

Applying Proposition 2.5 and projection measurement $\sum_{j^*}^{j^{**}} |j\rangle\langle j|$, we derive the desired result. \square

Remark 2.8. Let $\tau := \Delta t s(A) \|A\|_{\max}$. According to [37], Proposition 2.5 is valid for $\tau = \mathcal{O}(\log(1/\epsilon)/\log \log(1/\epsilon))$. By Lévy modulus [36], we know

$$\|\Delta W\|_{\max} = \mathcal{O}(\sqrt{\Delta t \log(1/\Delta t)}), \quad \text{almost surely.}$$

Then, for additive noise case, we have

$$\tau = \mathcal{O}(\Delta t \sqrt{\log(1/\Delta t)}/\Delta p).$$

We can set $\Delta t \sqrt{\log(1/\Delta t)}/\Delta p = \mathcal{O}(\log(1/\epsilon)/\log \log(1/\epsilon))$ to meet the requirement of Proposition 2.5.

Similarly, for the multiplicative noise case, we have

$$\tau = \mathcal{O}(\sqrt{\Delta t \log(1/\Delta t)}/\Delta p).$$

Let $\sqrt{\Delta t \log(1/\Delta t)}/\Delta p = \mathcal{O}(\log(1/\epsilon)/\log \log(1/\epsilon))$ and we will meet the requirement of Proposition 2.5.

2.5 Multi-sample Simulation

In practice, we need to compute multiple samples of the SDE to calculate, for example, the expectation of the solution. We can also directly apply the Schrödingerisation procedure for multiple samples simulation for SDE (1). Suppose we aim to simulate N samples, take

$$\tilde{A}_k = \begin{pmatrix} A & \cdots & 0 & B\Delta W_k^{(1)} & \cdots & 0 \\ \vdots & \ddots & \vdots & \vdots & \ddots & \vdots \\ 0 & \cdots & A & 0 & \cdots & B\Delta W_k^{(N)} \\ 0 & \cdots & \mathbf{0} & \mathbf{0} & \cdots & \mathbf{0} \end{pmatrix}, \quad \tilde{Y} = \begin{pmatrix} \tilde{X}^{(1)} \\ \vdots \\ \tilde{X}^{(N)} \\ 1/\Delta t \\ \vdots \\ 1/\Delta t \end{pmatrix}, \quad \tilde{Y}(0) = \begin{pmatrix} x_0 \\ \vdots \\ x_0 \\ 1/\Delta t \\ \vdots \\ 1/\Delta t \end{pmatrix},$$

where $\Delta W_k^{(j)} = W_{t_{k+1}}^{(j)} - W_{t_k}^{(j)}$ is the increment of the j -th sample path of the standard d -dimensional Brownian motion and $\tilde{X}^{(j)}$ is the j -th sample path of \tilde{X} . Here \tilde{A} is an $N(d+1) \times N(d+1)$ matrix and $\mathbf{0}$ represents the $N \times d$ zero matrix. Then we can follow exactly the same procedure to solve equation (4) with \tilde{A}_k and \tilde{Y} defined here. The sparsity of $(\tilde{A}_k + \tilde{A}_k^\dagger)$ is $(d+1)$ and thus the sparsity of $H_{1,k}$ and $H_{2,k}$ is $(d+1)$. So the gate complexity for N -samples simulation of SDE (1) is

$$N_{\text{Gates,Schr}} = \mathcal{O}\left(\frac{Td}{\Delta p} \left(\log\left(\frac{1}{\Delta p}\right) + \log(Nd)\right) \left(\|A\|_{\max} + \max_{1 \leq j \leq N} |\Delta W^{(j)}|_{\max} / \sqrt{\Delta t}\right)\right).$$

Similarly, for SDE (10), define

$$\tilde{A}_k = \begin{pmatrix} \tilde{A}_k^{(1)} & \cdots & 0 \\ \vdots & \ddots & \vdots \\ 0 & \cdots & \tilde{A}_k^{(N)} \end{pmatrix}, \quad \tilde{Y} = \begin{pmatrix} \tilde{X}^{(1)} \\ \vdots \\ \tilde{X}^{(N)} \end{pmatrix}, \quad \tilde{Y}(0) = \begin{pmatrix} x_0 \\ \vdots \\ x_0 \end{pmatrix}.$$

Here,

$$\tilde{A}_k^{(j)} = A - \frac{1}{2} \sum_{l=1}^m (B^{(l)})^2 + \sum_{l=1}^m B^{(l)} \frac{\Delta W_k^{(j,l)}}{\Delta t},$$

and $\Delta W_k^{(j)} = W_{t_{k+1}}^{(j)} - W_{t_k}^{(j)}$ is the increment of the j -th sample path of the standard m -dimensional Brownian motion $W^{(j)}$ and $\Delta W_k^{(j)} = (\Delta W_{k_{-1}}^{(j,1)}, \dots, W_k^{(j,m)})$. $\tilde{X}^{(j)}$ is the j -th sample path of \tilde{X} . The sparsity of \tilde{A}_k is d and the same holds for $(\tilde{A}_k + \tilde{A}_k^\dagger)$. So the gate complexity for N -samples simulation of SDE (10) is

$$N_{\text{gates,Schr}} = \mathcal{O}\left(\frac{Td}{\Delta p} \left(\log\left(\frac{1}{\Delta p}\right) + \log(Nd)\right) \left(\|A\|_{\max} + m\|B\|_{\max}^2 + \frac{m\|B\|_{\max} \max_{1 \leq j \leq N} |\Delta W^{(j)}|_{\max}}{\Delta t}\right)\right).$$

The computational complexity of the Euler-Maruyama scheme for simulating N samples of the d -dimensional SDE with additive Gaussian noise (1) is $\mathcal{O}(Nd^2T/\Delta t)$, so there is a quantum advantage when

$$\frac{Nd}{\log(Nd)} \gtrsim \frac{\Delta t}{\Delta p} \left(1 - \frac{\log(\Delta p)}{\log(Nd)}\right) \left(\|A\|_{\max} + \max_{1 \leq j \leq N} |\Delta W^{(j)}|_{\max} / \sqrt{\Delta t}\right).$$

The computation complexity of the Milstein scheme for simulating N samples of the d -dimensional SDE with multiplicative Gaussian noise (10) is $\mathcal{O}(Nmd^2T/\Delta t)$, so there is a quantum advantage when

$$\frac{Nd}{\log(Nd)} \gtrsim \frac{\sqrt{\Delta t}}{\Delta p} \left(1 - \frac{\log(\Delta p)}{\log(Nd)}\right) \left(\left(\frac{\|A\|_{\max}}{m} + \|B\|_{\max}^2\right) \sqrt{\Delta t} + \frac{\|B\|_{\max} \max_{1 \leq j \leq N} |\Delta W^{(j)}|_{\max}}{\sqrt{\Delta t}}\right).$$

3 Numerical experiments

In this section, we will apply the Schrödingerisation method to various SDEs in classical computers to illustrate the validation of the method in detail. Note that due to the no-cloning theorem, we can not compute the whole sample path in one run on the quantum computer. We present the computed sample path to illustrate the validation of our method.

Example 3.1 (The Ornstein–Uhlenbeck process). The Ornstein–Uhlenbeck process is a type of continuous-time stochastic process that finds applications in various fields such as physics [15], biology [22], stochastic analysis [14] and etc. Consider a one-dimensional Ornstein–Uhlenbeck process:

$$dX(t) = aX(t) dt + r dW_t, \quad X_0 = x_0, \quad 0 \leq t \leq T, \quad (23)$$

where a and r are constants.

The explicit solution to equation (23) is

$$X(t) = e^{at} \left(x_0 + r \int_0^t e^{-as} dW_s \right).$$

For the time mesh $\{t_j = j\Delta t : \Delta t = T/N_T, j = 0, 1, \dots, N_T - 1\}$, the explicit solution to the numerical formalism (3) in the k -th iteration is

$$\tilde{X}(t_{k+1}) = e^{a\Delta t} \tilde{X}(t_k) + (e^{a\Delta t} - 1) \frac{r\Delta W_k}{a\Delta t}. \quad (24)$$

In the following, we use $\sqrt{\Delta t}\xi_k$ to represent ΔW_k , where $\xi_k \sim N(0, 1)$ are independent standard Gaussian random variables. Take

$$\tilde{A}_k = \begin{pmatrix} a & r\xi_k \\ 0 & 0 \end{pmatrix}, \quad \tilde{Y} = \begin{pmatrix} \tilde{X}(t_k) \\ \frac{1}{\sqrt{\Delta t}} \end{pmatrix}, \quad \mathbf{v}(t, p) = \begin{pmatrix} v_1(t, p) \\ v_2(t, p) \end{pmatrix}. \quad (25)$$

The Hermitian matrices $H_{1,k}$ and $H_{2,k}$ in equation (14) then become

$$H_{1,k} = \begin{pmatrix} a & \frac{r}{2}\xi_k \\ \frac{r}{2}\xi_k & 0 \end{pmatrix}, \quad H_{2,k} = \begin{pmatrix} 0 & \frac{-ir}{2}\xi_k \\ \frac{ir}{2}\xi_k & 0 \end{pmatrix}.$$

For the normalized integration recovery formula (7) and (20), it is crucial to choose an appropriate recovery region U and the corresponding U_p . It is clear that with the negative diffusion term a and $r = 0$, the solution $v_1(t, p)$ of equation (14) will move from the right to the left in the $(p, v_1(t, p))$ plane. Because in this case the solution to equation (14) is

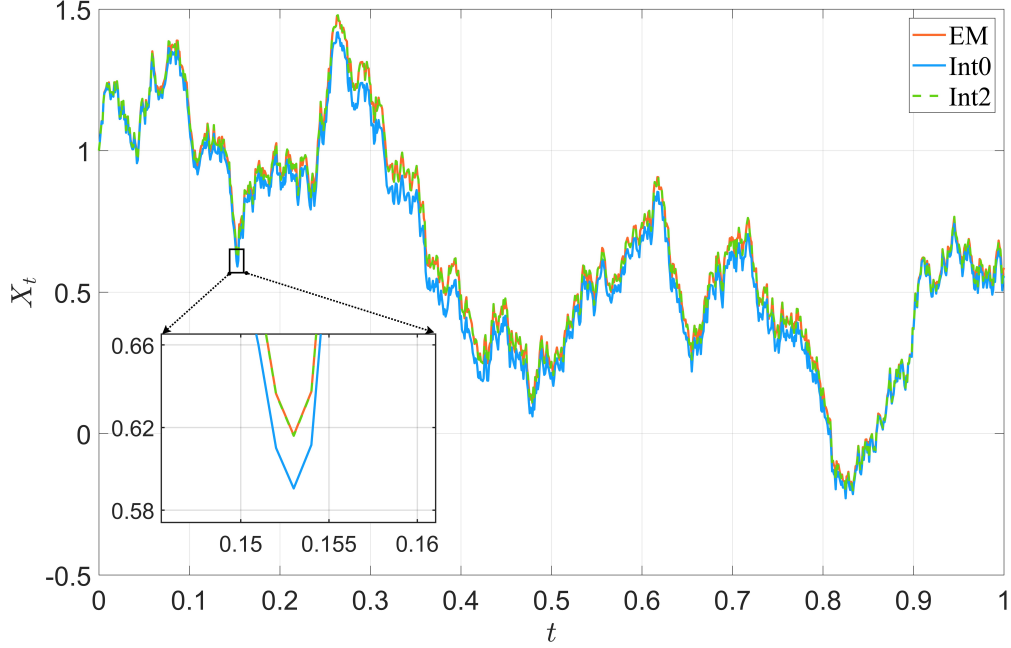
$$v_1(t, p) = \exp(-|p - at|)x_0.$$

So, for this no-noise case, it is sufficient to choose $U = [0, \infty)$ and $U_p = [0, R]$. However, due to the nature of the noise term $r\xi_k$, the noise term can take positive values, which in turn causes the maximum eigenvalue of matrix $H_{1,k}$ become positive. According to [24, Theorem 3.1], the left end-point of the recovery region should be chosen to be greater than 0, otherwise, an additional recovery error may arise. For $a > 0$, even for the no-noise case, recovering the numerical solution from the recovery region $U = [0, \infty)$ and $U_p = [0, R]$ will induce additional error. In figure 1, we shows the influence of the recovery region for SDE (23) with $a = 1$ and $r = 1$.

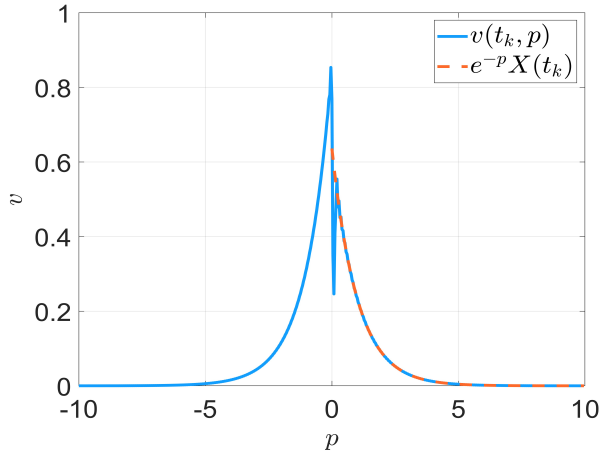
For $a < 0$, the largest positive eigenvalue of matrix $H_{1,k}$ is

$$\lambda_{\max}^+ = \frac{a + \sqrt{a^2 + r^2\xi^2/4}}{2} \leq \frac{|r\xi|}{4}.$$

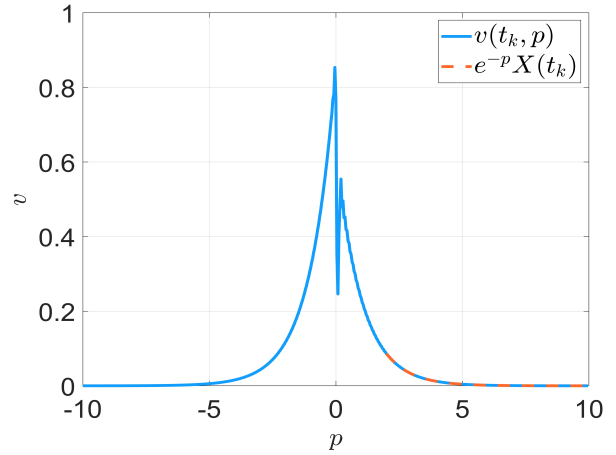
According to [24, Theorem 3.1], we can choose the left side of the recovery region $p^* > \lambda_{\max}^+ T$ with $p^* = |r\xi|/4$. By solving the ordinary differential equations (14) via second order i-stable Runge-Kutta method, we obtain the numerical solution \mathbf{c} and $\tilde{\mathbf{w}} = (\tilde{w}_1, \tilde{w}_2)$. Then we can recover the numerical solution $\tilde{X}^{\tilde{\mathbf{w}}}$ from



(a1)



(a2)



(a3)

Figure 1: $a = 1, r = 1, T = 1, \Delta t = 1 \times 10^{-3}, \Delta p = 0.04$ computed by i-stable second order Runge-Kutta method and recovered by the normalized integration method on interval $[2, 10]$. **(a1)**: A sample path of the solution; **(a2)**: The corresponding $v(t_k, p)$ and $e^{-p}X(t_k)$ with $t_k = 0.152$ on the recovery region $[0, 10]$; **(a3)**: The corresponding $v(t_k, p)$ and $e^{-p}X(t_k)$ with $t_k = 0.152$ on the recovery region $[2, 10]$.

| T | Δt | Δp | Int | Intp | EM |
|-----|--------------------|--------------------|-----------------------|-----------------------|-----------------------|
| 1 | 2×10^{-3} | 8×10^{-2} | 1.42×10^{-3} | 1.07×10^{-3} | 5.96×10^{-4} |
| 1 | 1×10^{-3} | 4×10^{-2} | 4.26×10^{-4} | 2.96×10^{-4} | 2.96×10^{-4} |
| 1 | 5×10^{-4} | 2×10^{-2} | 2.47×10^{-4} | 1.44×10^{-4} | 1.48×10^{-4} |

Table 1: Mean square error between the recovered solution $\tilde{X}^{\tilde{w}}$ and the approximate solution \tilde{X} for $a = -1$ and $\sigma = 1$, using 10^5 samples computed on a classical computer. The **Int** column is based on the normalized integration method on the fixed interval $[1.5, 10]$ of the p -axis. The **Intp** column is based on the normalized integration method on the fixed interval $[p^*, 10]$ of the p -axis. The **EM** column is the error between the solution \hat{X} of the Euler-Maruyama scheme and the approximate solution \tilde{X} .

\tilde{w}_1 based on the normalized integration method (20). We compute 10^5 samples and use the mean square error (MSE) which is

$$\text{MSE}(\tilde{X}^{\tilde{w}}(T), \tilde{X}(T)) \triangleq \sqrt{\mathbb{E}(|\tilde{X}^{\tilde{w}}(T) - \tilde{X}(T)|^2)},$$

where \tilde{X} is computed with the same set of random variables by formula (24). The results are shown in Table 1.

Example 3.2 (One dimensional Lévy flights). Lévy flights are a class of non-Gaussian stochastic process whose stationary increments satisfy a stationary distribution, which is heavy-tailed. Lévy flights find applications in a wide variety of fields, including optics [6], searching [43], earthquake behavior [10], etc.

Consider a one-dimensional Lévy flight described by the following the SDE

$$dX(t) = \mu X(t)dt + \sigma dL_t^\alpha, \quad (26)$$

where L_t^α is a one-dimensional symmetric α -stable Lévy motion. We can follow the same steps as the case of SDE with additive Gaussian noise, except for replacing the noise term as

$$\Delta L_k^\alpha \stackrel{d}{=} \Delta t^{\frac{1}{\alpha}} \xi_k$$

where $\xi_k \sim S(\alpha, 0, 0)$ is a symmetric stable random variable. Different from the case of the Gaussian noise, the Lévy process contains “large jumps” in its sample path, which means ΔL_k^α may become a fairly large number and influence the eigenvalues of the Hermitian matrix $\tilde{H}_{1,k}$. In this case, a smaller Δp will cause severe oscillation in the process of solving the ODE parts and significantly increase the error of the Schrödingerisation method. So we use the scale techniques in [24] to mitigate the impact off the large jumps. Define

$$\tilde{A}_k = \begin{pmatrix} \mu & \epsilon \sigma \Delta t^{\frac{1}{\alpha}} \xi_k \\ 0 & 0 \end{pmatrix}, \quad \tilde{Y}(t) = \begin{pmatrix} \tilde{X}(t) \\ \frac{1}{\epsilon \Delta t} \end{pmatrix}.$$

Then, applying the Schrödingerisation method in Section 2.1, we can compute the sample path of (26) using Hamiltonian simulation. We use the classical computer to compute 10^5 samples and use the mean absolute error (MAE):

$$\text{MAE}(X(T), Y(T)) = \mathbb{E}|X(T) - Y(T)|.$$

The result is shown in Table 2.

Example 3.3 (Geometric Brownian motion). Geometric Brownian motion is a continuous time stochastic process and is known for its application in the Black-Scholes model[7].

Consider the geometric Brownian motion described by the following one-dimensional stochastic differential equation

$$dX_t = \mu X_t dt + \sigma X_t dW_t, \quad X(0) = x_0 = 1. \quad (27)$$

The explicit solution to (27) is

$$X(t) = x_0 \exp\left(\left(\mu - \frac{1}{2}\sigma^2\right)t + \sigma W_t\right).$$

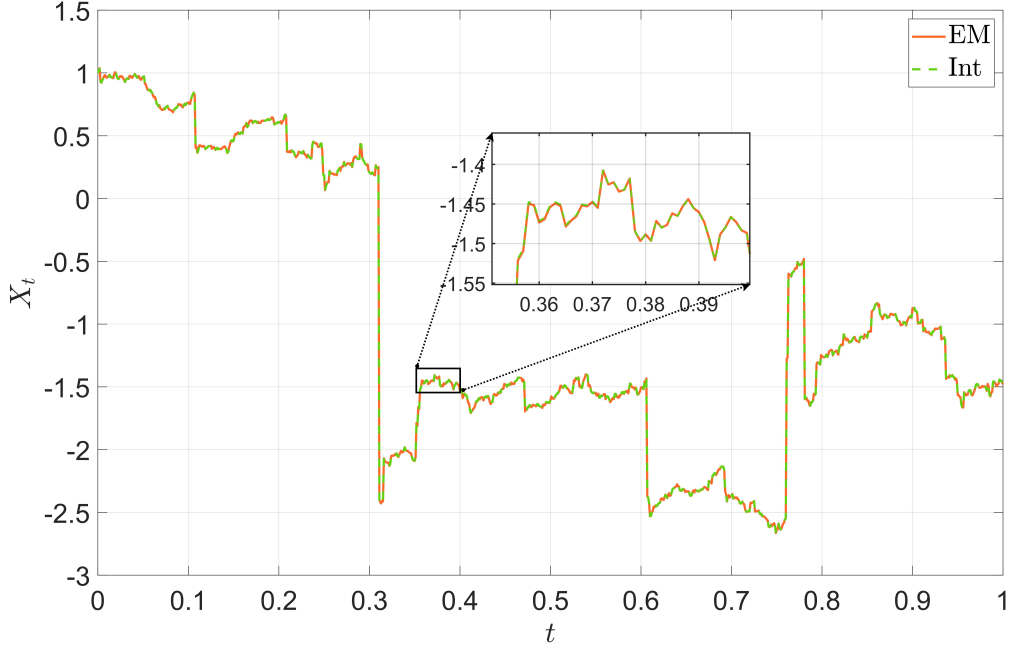


Figure 2: A Sample path of equation (26) for $\mu = -1, r = 1, T = 1, \Delta t = 1 \times 10^{-3}, \Delta p = 0.04$ computed by i-stable second order Runge-Kutta method and recovered by the normalized integration method and compared to the Euler-Maruyama solution. Large jumps take place near $t = 0.3, 0.6$ and 0.76 .

| T | Δt | Δp | Int | EM |
|-----|--------------------|--------------------|-----------------------|-----------------------|
| 1 | 2×10^{-3} | 8×10^{-2} | 2.20×10^{-3} | 7.72×10^{-4} |
| 1 | 1×10^{-3} | 4×10^{-2} | 6.45×10^{-4} | 3.95×10^{-4} |
| 1 | 5×10^{-4} | 2×10^{-2} | 2.97×10^{-4} | 1.99×10^{-4} |

Table 2: Mean absolute error compared to the approximate SDE for $\mu = -1, \sigma = 1, \alpha = 1.5$ and $\epsilon = 0.1$, using 10^5 samples computed on a classical computer. The **Int** column is the error between the recovered solution $\tilde{X}^{\tilde{w}}$ and the approximate solution \tilde{X} , which is based on the normalized integration method on the fixed interval $[1.5, 10]$ of the p -axis. The **EM** column is the error between the solution \hat{X} of the Euler-Maruyama scheme and the approximate solution \tilde{X} .

For the time mesh $\{t_j = j\Delta t : \Delta t = T/N_T, j = 0, 1, \dots, N_T - 1\}$, the corresponding ordinary differential equation (11) is

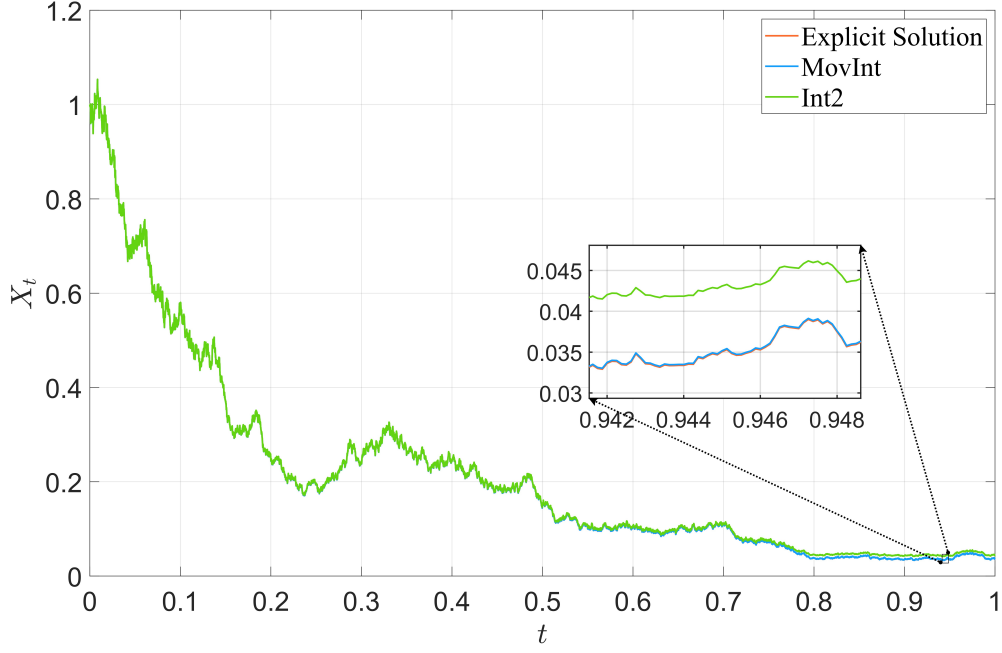
$$\begin{cases} \frac{d\tilde{X}(t)}{dt} = \tilde{A}_k \tilde{X}(t), & \tilde{X}(0) = x_0 \text{ and } t_k \leq t \leq t_{k+1}, \\ \tilde{A}_k = \mu - \frac{\sigma^2}{2} + \sigma \frac{\Delta W_k}{\Delta t}. \end{cases}$$

We use $\sqrt{\Delta t} \xi_k$ to represent ΔW_k and $H_{1,k}, H_{2,k}$ then becomes

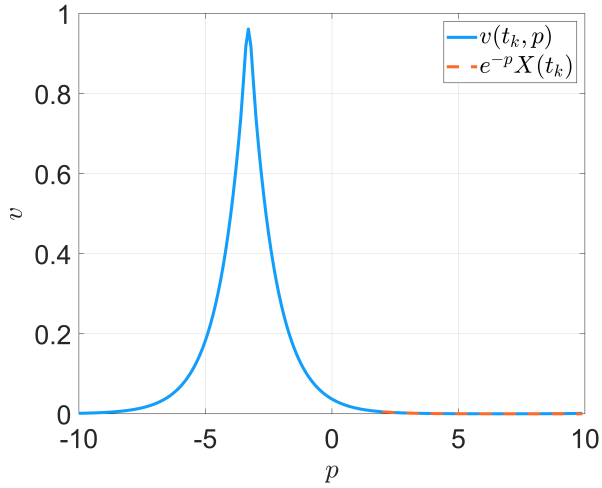
$$H_{1,k} = \tilde{A}_k = \mu - \frac{\sigma^2}{2} + \sigma \frac{\xi_k}{\sqrt{\Delta t}}, \quad H_{2,k} = 0.$$

We can follow exactly the same steps in the additive noise on interval $[-L, L]$ for mesh $p_j = L + (j-1)\Delta p$ with $\Delta p = (2L)/M$. It is also important to choose an appropriate recovery region U_p . In this example, we choose a “moving” U_p , that is, a time-dependent U_p . Let

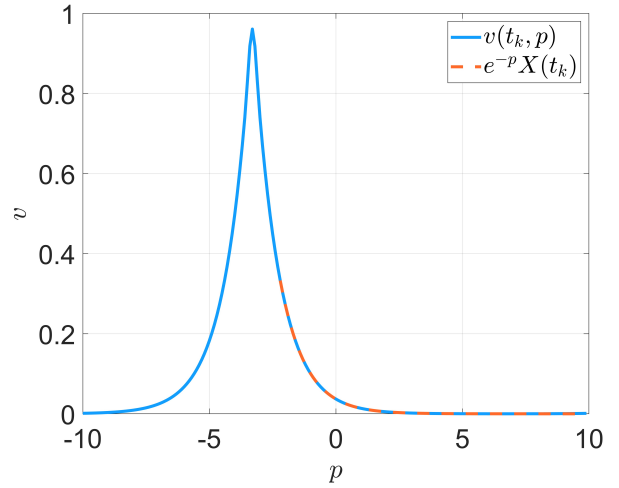
$$p^*(t) = \operatorname{argmax}\{v(t, p_j), 0 \leq j \leq M\}.$$



(a1)



(a2)



(a3)

Figure 3: $a = -1, r = 1, T = 1, \Delta t = 1.25 \times 10^{-4}, \Delta p = 0.01$ computed by i-stable second order Runge-Kutta method and recovered by the normalized integration method. **(a1)**: A sample path of the solution; **(a2)**: The corresponding $v(t_k, p)$ and $e^{-p}X(t_k)$ with $t_k = 0.9465$ on the fixed recovery region $[2, 10]$; **(a3)**: The corresponding $v(t_k, p)$ and $e^{-p}X(t_k)$ with $t_k = 0.9465$ on the moving recovery region $[p^*(t_k) + 1, 10]$;

We use the recovery region $U_p = [p^*(t) + 1, R]$ to implement the normalized integration method (20). The time-dependent recovery region U_p will move with the wave $v(t, p)$ and it will further reduce the recovery error. It is because the wave $v(t, p)$ shows less oscillation near the peak p^* . So we can choose the left end of the recovery region near the peak. Numerical results are shown in Table 3 for $\mu = -1, \sigma = 1$ and $T = 1$, using 10^5 samples computed on a classical computer.

| T | Δt | Δp | Int2 | MovInt | EM |
|-----|-----------------------|------------|-----------------------|-----------------------|-----------------------|
| 1 | 5×10^{-4} | 0.2 | 3.01×10^{-3} | 8.52×10^{-5} | 9.51×10^{-3} |
| 1 | 2.5×10^{-4} | 0.1 | 3.31×10^{-3} | 7.19×10^{-5} | 6.77×10^{-3} |
| 1 | 1.25×10^{-4} | 0.05 | 1.20×10^{-2} | 7.28×10^{-5} | 4.97×10^{-3} |

Table 3: Mean square error compared to the explicit solution of SDE (27) for $\mu = -1$ and $\sigma = 1$, using 10^5 samples computed on a classical computer. The error in the **Int2** column is based on the normalized integration method on the fixed interval $[2, 10]$ of the p -axis. The error in the **MovInt** column is based on the normalized integration method on the moving interval $[p^* + 1, 10]$ of the p -axis. The **EM** column is the error between the solution \hat{X} of the Euler-Maruyama scheme and the explicit solution X .

In Table 3, the error based on recovering from the fixed region $[2, 10]$ (The **Int2** column) does not decrease along with Δt and Δp . It is because the recovery region does not cover the essential part of the wave function $v(t, p)$ and it will cause an additional error that can not be improved by decreasing Δt and Δp . However, by choosing the recovery region starting near the peak, the performance of the scheme is significantly improved as it is shown in the **MovInt** column.

4 Analysis on convergence rate

In this section, we will give the proof of the convergence rate of the Schrödingerisation procedure for both SDE with additive Gaussian noise and multiplicative Gaussian noise. Specifically, we will show the mean square error between the analytical solution $X(T)$ of equation (1) and equation (10) between their corresponding numerical solution $\tilde{X}^{\tilde{w}}(T)$. We have

$$\|X(T) - \tilde{X}^{\tilde{w}}(T)\|_2 \leq \|X(T) - \tilde{X}(T)\|_2 + \sqrt{\mathbb{E}\|\tilde{X}(T) - \tilde{X}^{\tilde{w}}(T)\|^2}, \quad (28)$$

where \tilde{X} is the analytical solution of the approximate equation (3) and (11). Here we use $\|\cdot\|_2 = \sqrt{\mathbb{E}\|\cdot\|^2}$ to denote the mean square norm, where $\|\cdot\|$ is the Euclidean norm for vectors and operator norm for matrices. It is clear that $\|X(T) - \tilde{X}(T)\|_2$ is the error between the approximate equation and the SDE, and error $\|\tilde{X}(T) - \tilde{X}^{\tilde{w}}(T)\|$ comes from the recovery part.

Denote $H_1(t) = \sum_{k=0}^{N_T-1} H_{1,k} \mathbb{1}_{[t_k, t_{k+1})}(t)$, $\lambda_{\max}^-(H_1) = |\min_{t \in [0, T]} \{\lambda(H_1(t)), 0\}|$ and $I = [-L, L]$. We use $\|\cdot\|_{L^2(I)}$ and $\|\cdot\|_{H^1(I)}$ to denote the L^2 -norm and H^1 -norm on interval I of variable p .

Assumption H1. Assume the eigenvalues of H_1 has the following order

$$\lambda_1(H_1) \leq \lambda_2(H_1) \leq \cdots \leq \lambda_d(H_1), \quad \text{for all } t \in [0, T].$$

Assumption H2. Assume the interval $I = [-L, L]$ satisfies

$$L \geq \max\{\lambda_{\max}^-(H_1)T, p^*\}.$$

where $p^* \geq \max\{\lambda_{\max}(H_1)T, 0\}$ and $\lambda_{\max}(H_1) = \max_{0 \leq t \leq T} \lambda(H_1(t))$.

We have the following results.

Theorem 4.1. *For the d -dimensional SDE with additive Gaussian noise (1), suppose the recovery region U_p is properly chosen, which means the solution to (5) satisfies $v(t, p) = e^{-p\tilde{Y}(t)}$ for $p \in U_p$. Suppose the*

Assumption **H1** and **H2** are satisfied. Then, the mean square norm between the recovered solution $\tilde{X}^{\tilde{w}}(T)$ and the solution $X(T)$ of the SDE (1) satisfies

$$\|X(T) - \tilde{X}^{\tilde{w}}(T)\|_2 \lesssim C_2 \Delta t + (\Delta p^{\frac{3}{2}} + \sqrt{T} e^{-L} \tilde{C}) \|\tilde{Y}(0)\| \quad (29)$$

where $C_2 = \sqrt{dc_1(e^{2\|A\|T} - 1)/(2\|A\|)}$ with $c_1 = \max_{1 \leq l \leq d} |AB^{(l)}|^2$ and

$$\tilde{C} = \sqrt{\mathbb{E} \left[|\lambda_{\max}^-(H_1)|^2 e^{2\lambda_{\max}^-(H_1)} \right]}.$$

Proof. The proof follows directly from inequality (28), Lemma 4.3, Proposition 4.5 and Proposition 4.7. \square

Similarly, for the SDE with multiplicative Gaussian noise, we have the following result.

Theorem 4.2. For the d -dimensional SDE with multiplicative Gaussian noise (10), suppose the recovery region U_p is properly chosen, which means the solution to (14) satisfies $\mathbf{v}(t, p) = e^{-p} \tilde{X}(t)$ for $p \in U_p$. Further suppose the Assumption **H1** and **H2** are satisfied. Then, the mean square norm between the recovered solution $\tilde{X}^{\tilde{w}}(T)$ and the solution $X(T)$ of the SDE (10) satisfies

$$\|X(T) - \tilde{X}^{\tilde{w}}(T)\|_2 \lesssim \Delta t + (\Delta p^{\frac{3}{2}} + \sqrt{T} e^{-L} \tilde{C}) \|\tilde{X}(0)\|, \quad (30)$$

where

$$\tilde{C} = \sqrt{\mathbb{E} \left[|\lambda_{\max}^-(H_1)|^2 e^{2\lambda_{\max}^-(H_1)} \right]}.$$

Proof. The proof follows directly from inequality (28), Lemma 4.3, Proposition 4.5 and Proposition 4.8. \square

For $0 \leq k \leq N_T$, let $\tilde{\mathbf{w}}^c(t_k, p) = [\tilde{w}_1(t, p), \dots, \tilde{w}_d(t_k, p)]$ where $\tilde{w}_h(t_k, p) = \sum_{l=1}^{2N} c_l^{(h)}(t) e^{i\mu_l(p+L)}$ with $c_l^{(h)}$ solved in equation (16).

Lemma 4.3. For \mathbf{v} governed by equation (14), the H^1 -estimate of \mathbf{v} satisfies

$$\|\mathbf{v}(t_k, \cdot)\|_{H^1(I)} \leq \sqrt{2} \|z_0\|, \quad 0 \leq k \leq N_T.$$

Proof. We first show that

$$\|\mathbf{v}(t_k, \cdot)\|_{H^1(I)} \leq \|\mathbf{v}(0, \cdot)\|_{H^1(\mathbb{R})}. \quad (31)$$

It is clear that $\|\mathbf{v}(t_{k+1}, \cdot)\|_{H^1(I)}^2 \leq \|\mathbf{v}(t_{k+1}, \cdot)\|_{H^1(\mathbb{R})}^2$. So, we only need to prove $\|\mathbf{v}(t_{k+1}, \cdot)\|_{H^1(\mathbb{R})}^2 = \|\mathbf{v}(t_k, \cdot)\|_{H^1(\mathbb{R})}^2$. Recall that $\mathbf{v}(t, p)$ satisfies equation (14) for $p \in (-\infty, \infty)$ and its Fourier transformation $w(t, \eta)$ satisfies (6). As matrices $H_{1,k}$ and $H_{2,k}$ are Hermite matrices, the solution operator $\exp(-i(\eta H_{1,k} + H_{2,k})\Delta t)$ is a unitary matrix. It means, for every η ,

$$\|w(t_{k+1}, \eta)\| = \|\exp(-i(\eta H_{1,k} + H_{2,k})\Delta t) w(t_k, \eta)\| = \|w(t_k, \eta)\|.$$

We know that

$$\begin{aligned} \|\mathbf{v}(t_{k+1}, \cdot)\|_{H^1(\mathbb{R})}^2 &= \|\mathbf{v}(t_{k+1}, \cdot)\|_{L^2(\mathbb{R})}^2 + \|\partial_p \mathbf{v}(t_{k+1}, \cdot)\|_{L^2(\mathbb{R})}^2 \\ &= \|w(t_{k+1}, \cdot)\|_{L^2(\mathbb{R})}^2 + \int_{\mathbb{R}} \|-i\eta w(t_{k+1}, \eta)\|^2 d\eta \\ &= \|w(t_k, \cdot)\|_{L^2(\mathbb{R})}^2 + \int_{\mathbb{R}} \|-i\eta w(t_k, \eta)\|^2 d\eta \\ &= \|\mathbf{v}(t_k, p)\|_{H^1(\mathbb{R})}^2. \end{aligned}$$

With the definition of $\mathbf{v}(0)$, we also have

$$\|\mathbf{v}(0)\|_{H^1(\mathbb{R})} = \|z_0\| \sqrt{\int_{\mathbb{R}} e^{-2|p|} + \left| \frac{\partial}{\partial p} e^{-|p|} \right|^2 dp} = \sqrt{2} \|z_0\|.$$

Combining with equation (31), we obtain the desired result. \square

The following lemma follows from [24, Theorem 4.1] and Lemma 4.3. It shows the L^2 error between $\tilde{\mathbf{w}}^c$ and \mathbf{v} .

Lemma 4.4. *Suppose the Assumption H1 and H2 are satisfied. For the numerical solution $\tilde{\mathbf{w}}$ of equation (19) and the solution \mathbf{v} of equation (14) on $[0, T] \times I$, it holds*

$$\|\tilde{\mathbf{w}}^c(t_k, \cdot) - \mathbf{v}(t_k, \cdot)\|_{L^2(I)} \lesssim \left(\Delta p + \sqrt{\frac{|\lambda_{\max}^-(H_1)|^2 t_k}{\Delta p}} e^{\lambda_{\max}^-(H_1) - L} \right) \|\tilde{Y}(0)\|.$$

The following proposition gives the error rate for recovering solution \tilde{X} .

Proposition 4.5 (Recovery error analysis). *Suppose the recovery region U_p is properly chosen, which means the solution to (6) satisfies $w(t, p) = e^{-p}\tilde{Y}(t)$ for $p \in U_p$. Further assume the Assumption H1 and H2 are satisfied. Then, the Euclidean distance between the recovered solution $\tilde{X}^{\tilde{\mathbf{w}}}(t_k)$ and the solution $\tilde{X}(t_k)$ of the approximate equation (3) satisfies*

$$\|\tilde{X}^{\tilde{\mathbf{w}}}(t_k) - \tilde{X}(t_k)\| \lesssim \left(\Delta p^{\frac{3}{2}} + \sqrt{|\lambda_{\max}^-(H_1)|^2 t_k} e^{\lambda_{\max}^-(H_1) - L} \right) \|\tilde{Y}(0)\|. \quad (32)$$

Proof. We only need to show

$$\|\tilde{X}^{\tilde{\mathbf{w}}}(t_k) - \tilde{X}(t_k)\|^2 \lesssim \Delta p \|\tilde{\mathbf{w}}^c(t_k, \cdot) - \mathbf{v}(t_k, \cdot)\|_{L^2(I)}^2. \quad (33)$$

Then, by Lemma 4.3 and Lemma 4.4, we get the desired estimate (32). Note that $\|\tilde{X}^{\tilde{\mathbf{w}}}(t_k) - \tilde{X}(t_k)\|^2 = \sum_{h=1}^d |\tilde{X}_h^{\tilde{\mathbf{w}}}(t_k) - \tilde{X}_h(t_k)|^2$ in (32) is a random variable. It means that every computed sample of the SDE can be bounded by the right hand side of inequality (32).

Now we continue to prove estimate (33). As $\mathbf{v}(t, p) = e^{-p}\tilde{Y}(t)$ for $p \in U_p$, it is clear that

$$\tilde{Y}(t_k) = \begin{pmatrix} \tilde{X}(t_k) \\ 1/\Delta t \end{pmatrix} = \frac{\int_{U_p} \mathbf{v}(t_k, p) dp}{\int_{U_p} e^{-p} dp} = \frac{\sum_{p_j \in U_p} \mathbf{v}(t_k, p_j) \Delta p}{\sum_{p_j \in U_p} e^{-p_j} \Delta p}.$$

Then the error between the solution $\tilde{X}(t)$ of the approximate equation (3) and the numerical solution $\tilde{X}^{\tilde{\mathbf{w}}}(t)$ of equation (20) is

$$\begin{aligned} \|\tilde{X}^{\tilde{\mathbf{w}}}(t_k) - \tilde{X}(t_k)\|^2 &= \sum_{h=1}^d |\tilde{X}_h^{\tilde{\mathbf{w}}}(t_k) - \tilde{X}_h(t_k)|^2 \\ &\leq \frac{2}{\left(\sum_{p_j \in U_p} e^{-p_j}\right)^2} \sum_{h=1}^d \sum_{p_j \in U_p} (\tilde{w}_h(t_k, p_j) - v_h(t_k, p_j))^2. \end{aligned}$$

In the last inequality, we used the fact that the first d -components of $\tilde{\mathbf{w}}$ and \mathbf{v} encode the value of $\tilde{X}^{\tilde{\mathbf{w}}}(t_k)$ and $\tilde{X}(t_k)$ respectively. Choose $U_p = [p^*, p^{**}] = [j_1 \Delta p, j_2 \Delta p]$, then

$$\begin{aligned} \frac{1}{\sum_{p_j \in U_p} e^{-p_j}} &= \frac{1}{\sum_{j=j_1}^{j_2-1} e^{-p_j}} \\ &= \frac{1 - e^{-\Delta p}}{e^{-j_1 \Delta p} - e^{-j_2 \Delta p}} = \frac{\Delta p}{1 - e^{-(j_2 - j_1) \Delta p}} e^{j_1 \Delta p} + \mathcal{O}(\Delta p^2). \end{aligned}$$

For $\mu_l = \pi(l - N - 1)/L$ and $p_j = -L + (j - 1)\Delta p$, a direct computation shows

$$\int_{-L}^L \left(\sum_{l=1}^{2N} \hat{u}_l e^{i\mu_l(p+L)} \right)^2 dp = 2L \sum_{l=1}^{2N} \hat{u}_l^2 = \sum_{j=1}^{2N} \left(\sum_{l=1}^{2N} \hat{u}_l e^{i\mu_l(p_j+L)} \right)^2 \Delta p,$$

and

$$\begin{aligned}
\frac{1}{2L} \sum_{j=1}^{2N} \left(\sum_{l=-\infty}^{\infty} \hat{u}_l e^{i\mu_l(p_j+L)} \right)^2 \Delta p &= \frac{1}{2L} \sum_{j=1}^{2N} \left(\sum_{l=1}^{2N} \sum_{\tau=-\infty}^{\infty} (\hat{u}_{l+2\tau N}) e^{i\mu_l(p_j+L)} \right)^2 \Delta p \\
&= \sum_{l=1}^{2N} \left(\sum_{\tau=-\infty}^{\infty} \hat{u}_{l+2\tau N} \right)^2 \\
&\leq 2 \sum_{l=-\infty}^{\infty} |\hat{u}_l|^2 = 2 \left\| \sum_{l=-\infty}^{\infty} \hat{u}_l e^{i\mu_l(p+L)} \right\|_{L^2(I)}^2.
\end{aligned}$$

Then

$$\begin{aligned}
\sum_{p_j \in U_p} (\tilde{w}_h(t_k, p_j) - v_h(t_k, p_j))^2 \Delta p &\leq \sum_{j=1}^{2N} (\tilde{w}_h(t_k, p_j) - v_h(t_k, p_j))^2 \Delta p \\
&\leq 4L \|\tilde{w}_h(t_k) - v_h(t_k)\|_{L^2(I)}^2.
\end{aligned}$$

Here we used the fact that

$$v_h(t_k, p_j) = \sum_{l=-\infty}^{\infty} \hat{v}_l^{(h)}(t_k) e^{i\mu_l(p_j+L)}, \quad \hat{v}_l^{(h)}(t_k) = \frac{1}{2L} \int_{-L}^L v_h(t_k, p) e^{-i\mu_l(p+L)} dp,$$

and

$$\tilde{w}_h(t_k, p_j) = \sum_{l=1}^{2N} c_l^{(h)}(t) e^{i\mu_l(p_j+L)} = \sum_{l=-\infty}^{\infty} c_l^{(h)}(t) e^{i\mu_l(p_j+L)}, \quad \text{with } c_l^{(h)} = 0 \text{ for } l \neq 1, \dots, 2N.$$

Then, we know

$$\begin{aligned}
\|\tilde{X}^{\tilde{w}}(t_k) - \tilde{X}(t_k)\|^2 &= \sum_{h=1}^d |\tilde{X}_h^{\tilde{w}}(t_k) - \tilde{X}_h(t_k)|^2 \\
&\leq \frac{2}{\left(\sum_{p_j \in U_p} e^{-p_j}\right)^2} \sum_{h=1}^d \sum_{p_j \in U_p} (\tilde{w}_h(t_k, p_j) - v_h(t_k, p_j))^2 \\
&\leq \frac{8L(1 - e^{-\Delta p})}{(e^{-j_1 \Delta p} - e^{-j_2 \Delta p})^2} \sum_{h=1}^d \|\tilde{w}_h(t_k) - v_h(t_k)\|_{L^2(I)}^2 + \mathcal{O}(\Delta p^2) \\
&\lesssim \Delta p \|\tilde{w}^c(t_k, \cdot) - v(t_k, \cdot)\|_{L^2(I)}^2.
\end{aligned}$$

□

Proposition 4.6. *In one-dimension, the estimate*

$$\|\tilde{X}(T) - X(T)\|_2 \leq C_1 \Delta t,$$

holds for the solution \tilde{X} of the approximate equation (3), where X is the solution of SDE (23) and $C_1 = |r| \sqrt{2a(e^{2aT} - 1)}/4$.

Proof. Recall that the solution to the one-dimensional SDE (23) is

$$X(t) = e^{at} \left(x_0 + r \int_0^t e^{-as} dW_s \right),$$

then

$$X(t_{k+1}) = e^{a\Delta t} X(t_k) + r \int_{t_k}^{t_{k+1}} e^{a(t_{k+1}-s)} dW_s.$$

The solution to the corresponding approximate equation (3) is

$$\tilde{X}(t_{k+1}) = e^{a\Delta t} \tilde{X}(t_k) + (e^{a\Delta t} - 1) \frac{r\Delta W_k}{a\Delta t} = e^{a\Delta t} \tilde{X}(t_k) + r \int_{t_k}^{t_{k+1}} \frac{e^{a\Delta t} - 1}{a\Delta t} dW_s.$$

We have

$$\begin{aligned} \mathbb{E}(\tilde{X}(t_{k+1}) - X(t_{k+1}))^2 &= e^{2a\Delta t} \mathbb{E}(\tilde{X}(t_k) - X(t_k))^2 + r^2 \mathbb{E} \left[\int_{t_k}^{t_{k+1}} e^{a(t_{k+1}-s)} - \frac{e^{a\Delta t} - 1}{a\Delta t} dW_s \right]^2 \\ &\quad + 2re^{a\Delta t} \mathbb{E} \left[(\tilde{X}(t_k) - X(t_k)) \int_{t_k}^{t_{k+1}} e^{a(t_{k+1}-s)} - \frac{e^{a\Delta t} - 1}{a\Delta t} dW_s \right] \\ &= e^{2a\Delta t} \mathbb{E}(\tilde{X}(t_k) - X(t_k))^2 + r^2 \int_{t_k}^{t_{k+1}} (e^{a(t_{k+1}-s)} - \frac{e^{a\Delta t} - 1}{a\Delta t})^2 ds. \end{aligned}$$

In the last equality, we used the Itô Isometry and the independence between the stochastic integral and the difference $\tilde{X}(t_k) - X(t_k)$. For $|a|\Delta t \ll 1$ and the fact that

$$\max_{0 \leq s \leq \Delta t} \left| e^{a(\Delta t-s)} - \frac{e^{a\Delta t} - 1}{a\Delta t} \right| = \max \left\{ \left| e^{a\Delta t} - \frac{e^{a\Delta t} - 1}{a\Delta t} \right|, \left| \frac{e^{a\Delta t} - 1}{a\Delta t} - 1 \right| \right\} = \frac{1}{2}|a|\Delta t + \mathcal{O}(\Delta t^2),$$

we have

$$\begin{aligned} \mathbb{E}(\tilde{X}(t_{k+1}) - X(t_{k+1}))^2 &\leq e^{2a\Delta t} \mathbb{E}(\tilde{X}(t_k) - X(t_k))^2 + r^2 \int_0^{\Delta t} \frac{1}{4} a^2 \Delta t^2 ds + \mathcal{O}(\Delta t^3) ds \\ &= e^{2a\Delta t} \mathbb{E}(\tilde{X}(t_k) - X(t_k))^2 + \frac{1}{4} (ar)^2 \Delta t^3 + \mathcal{O}(\Delta t^4). \end{aligned}$$

Let b_k denote $\mathbb{E}(\tilde{X}(t_k) - X(t_k))^2$, and the above inequality gives

$$b_{k+1} \leq e^{2a\Delta t} b_k + \frac{1}{4} (ar)^2 \Delta t^3 + \mathcal{O}(\Delta t^4).$$

Then we have

$$b_n \leq e^{2an\Delta t} b_0 + \sum_{k=0}^{n-1} e^{2ak\Delta t} \left(\frac{1}{4} (ar)^2 \Delta t^3 + \mathcal{O}(\Delta t^4) \right).$$

Given $b_0 = 0$, which means $X(0) = \tilde{X}(0)$, one has

$$b_n \leq \frac{(e^{2an\Delta t} - 1)}{4(e^{2a\Delta t} - 1)} ((ar)^2 \Delta t^3 + \mathcal{O}(\Delta t^4)).$$

Take $n = N_T$, $T = N_T \Delta t$ and $e^{2a\Delta t} - 1 = 2a\Delta t + \mathcal{O}((a\Delta t)^2)$,

$$b_{N_T} \leq \frac{r^2 a (e^{2aT} - 1) \Delta t^2}{8} + \mathcal{O}(\Delta t^3).$$

Then

$$\max_{t_k} \|\tilde{X}(t_k) - X(t_k)\|_2 \leq \|\tilde{X}(T) - X(T)\|_2 \leq \frac{|r| \sqrt{2a(e^{2aT} - 1)} \Delta t}{4} + \mathcal{O}(\Delta t^{\frac{3}{2}}).$$

It means that the solution of the approximate equation (3) converges to the solution of equation (23) with error rate $\mathcal{O}(\Delta t)$ under mean square norm. \square

We will next show the convergence rate for the d -dimensional case.

Consider the d -dimensional SDE

$$dX(t) = AX(t) dt + B dW_t = AX(t) dt + \sum_{l=1}^d B^{(l)} dW_t^{(l)}, \quad X_0 = x_0, \quad (34)$$

where A is a $d \times d$ matrix, $\{B^{(l)}\}$ is a group of $d \times 1$ vector and $\{W^{(l)}\}$ is a group of independent scalar standard Brownian motion. Here, we use the notation that $B = (B^{(1)}, \dots, B^{(d)})$ and $W_t = (W^{(1)}, \dots, W^{(d)})^\top$.

Proposition 4.7. For the d -dimensional SDE with additive Gaussian noise (34), the estimate

$$\|\tilde{X}(T) - X(T)\|_2 \leq C_2 \Delta t,$$

holds for the solution \tilde{X} of the approximate equation (3), where $C_2 = \sqrt{dc_1(e^{2\|A\|T} - 1)/(2\|A\|)}$ and $c_1 = \max_{1 \leq l \leq d} \|AB^{(l)}\|^2$.

Proof. According to [31, Ch 4.8], the solution to (34) is

$$X(t) = e^{At}x_0 + \int_0^t e^{A(t-s)}B dW_s = e^{At}x_0 + \sum_{l=1}^d \int_0^t e^{A(t-s)}B^{(l)} dW_s^{(l)}$$

For the corresponding approximate equation (3), by the Duhamel principle, one gets

$$\tilde{X}(t_{k+1}) = e^{A\Delta t}\tilde{X}(t_k) + \int_{t_k}^{t_{k+1}} e^{A(t_{k+1}-s)}\frac{B\Delta W_k}{\Delta t} ds = e^{A\Delta t}\tilde{X}(t_k) + \sum_{l=1}^d \int_{t_k}^{t_{k+1}} e^{A(t_{k+1}-s)}\frac{B^{(l)}\Delta W_k^{(l)}}{\Delta t} ds.$$

Therefore,

$$\begin{aligned} \mathbb{E}\|\tilde{X}(t_{k+1}) - X(t_{k+1})\|^2 &= \mathbb{E}\|e^{A\Delta t}(\tilde{X}(t_k) - X(t_k))\|^2 + \sum_{l=1}^d \mathbb{E}\left\|\int_{t_k}^{t_{k+1}} \int_0^{\Delta t} \frac{e^{A(\Delta t-s)}B^{(l)}}{\Delta t} - \frac{e^{A(t_{k+1}-\tau)}B^{(l)}}{\Delta t} ds dW_\tau\right\|^2 \\ &\quad + 2\mathbb{E}\left[\left(e^{A\Delta t}(\tilde{X}(t_k) - X(t_k))\right)^\dagger \sum_{l=1}^d \int_{t_k}^{t_{k+1}} \int_0^{\Delta t} \frac{e^{A(\Delta t-s)}B^{(l)}}{\Delta t} - \frac{e^{A(t_{k+1}-\tau)}B^{(l)}}{\Delta t} ds dW_\tau\right] \\ &= e^{2\|A\|\Delta t}\mathbb{E}\|\tilde{X}(t_k) - X(t_k)\|^2 + \sum_{l=1}^d \mathbb{E}\int_0^{\Delta t} \left\|\int_0^{\Delta t} \frac{e^{A(\Delta t-s)}B^{(l)}}{\Delta t} - \frac{e^{A(\Delta t-\tau)}B^{(l)}}{\Delta t} ds\right\|^2 d\tau. \end{aligned}$$

In the last equality, we used the Itô Isometry and the independence between the stochastic integral and the difference $\tilde{X}(t_k) - X(t_k)$. Here we use $\|\cdot\|$ to denote the vector norm. By the definition of the matrix exponential, for $\tau \in [0, \Delta t]$ and $\|A\|\Delta t \ll 1$, one has

$$\begin{aligned} &\left\|\int_0^{\Delta t} \frac{e^{A(\Delta t-s)}B^{(l)}}{\Delta t} - \frac{e^{A(\Delta t-\tau)}B^{(l)}}{\Delta t} ds\right\|^2 \\ &= \frac{1}{\Delta t^2} \left\|\int_0^{\Delta t} \left(\mathbf{I}_d + A(\Delta t - s) + \frac{1}{2}A^2(\Delta t - s)^2 + \mathcal{O}(\Delta t^3)\right)B^{(l)}\right. \\ &\quad \left. - \left(\mathbf{I}_d + A(\Delta t - \tau) + \frac{1}{2}A^2(\Delta t - \tau)^2 + \mathcal{O}(\Delta t^3)\right)B^{(l)} ds\right\|^2 \\ &= \frac{1}{\Delta t^2} \left\|\int_0^{\Delta t} \left(A(\tau - s) + \frac{1}{2}A^2(\tau - s)(2\Delta t - \tau - s) + \mathcal{O}(\Delta t^3)\right)B^{(l)} ds\right\|^2 \\ &= \frac{1}{\Delta t^2} \left\|AB^{(l)} \int_0^{\Delta t} (\tau - s)ds + A^2B^{(l)} \int_0^{\Delta t} (\tau - s)(2\Delta t - \tau - s)ds + \mathcal{O}(\Delta t^4)\right\|^2 \\ &\leq \frac{1}{2}\|AB^{(l)}\|^2\Delta t^2 + \frac{2}{9}\|A^2B^{(l)}\|^2\Delta t^4 + \mathcal{O}(\Delta t^6). \end{aligned}$$

Then, take $c_1 = \max_{1 \leq l \leq d} \frac{1}{2}\|AB^{(l)}\|^2$ and $c_2 = \max_{1 \leq l \leq d} \frac{2}{9}\|A^2B^{(l)}\|^2$, we have

$$\mathbb{E}\|\tilde{X}(t_{k+1}) - X(t_{k+1})\|^2 \leq e^{2\|A\|\Delta t}\mathbb{E}\|\tilde{X}(t_k) - X(t_k)\|^2 + d(c_1\Delta t^3 + c_2\Delta t^5 + \mathcal{O}(\Delta t^7)).$$

Similarly as the one-dimensional case, take $b_k = \mathbb{E} \|\tilde{X}(t_k) - X(t_k)\|^2$

$$\begin{aligned} b_{k+1} &\leq e^{2\|A\|\Delta t} b_k + dc_1 \Delta t^3 + \mathcal{O}(\Delta t^5) \\ &= e^{2(k+1)\|A\|\Delta t} b_0 + d \sum_{m=0}^k e^{2m\|A\|\Delta t} (c_1 \Delta t^3 + \mathcal{O}(\Delta t^5)) \\ &= \frac{dc_1 (e^{2(k+1)\|A\|\Delta t} - 1)}{e^{2\|A\|\Delta t} - 1} (\Delta t^3 + \mathcal{O}(\Delta t^5)). \end{aligned}$$

Take $T = N_T \Delta t$ and $e^{2\|A\|\Delta t} - 1 = 2\|A\|\Delta t + \mathcal{O}(\|A\|\Delta t)^2$, one has

$$b_{N_T} \leq \frac{dc_1 (e^{2\|A\|T} - 1)}{2\|A\|} \Delta t^2 + \mathcal{O}(\Delta t^4).$$

It means

$$\max_{t_k} \|\tilde{X}(t_k) - X(t_k)\|_2 \leq \|\tilde{X}(T) - X(T)\|_2 \leq \sqrt{\frac{dc_1 (e^{2\|A\|T} - 1)}{2\|A\|}} \Delta t + \mathcal{O}(\Delta t^2).$$

In d -dimensions, the solution of the approximate equation (3) converges to the solution of equation (23) with error rate $\mathcal{O}(\sqrt{d}\Delta t)$ under mean square norm. \square

In the following, we will move on to show the convergence rate for the SDE with multiplicative Gaussian noise.

Recall the SDE with multiplicative Gaussian noise:

$$dX(t) = AX(t)dt + \sum_{l=1}^m B^{(l)}X(t)dW_t^{(l)}, \quad X_0 = x_0, \quad (35)$$

$$\begin{cases} \frac{d\tilde{X}(t)}{dt} = \tilde{A}_k \tilde{X}(t), & \tilde{X}(0) = x_0 \text{ and } t_k \leq t \leq t_{k+1}, \\ \tilde{A}_k = A - \frac{1}{2} \sum_{l=1}^m (B^{(l)})^2 + \sum_{l=1}^m B^{(l)} \frac{\Delta W_k^{(l)}}{\Delta t}. \end{cases} \quad (36)$$

Here, $W_t = (W_t^{(1)}, \dots, W_t^{(m)})$ is a m -dimensional standard Brownian motion and $\Delta W_k^{(l)} = W_{t_{k+1}}^{(l)} - W_{t_k}^{(l)}$. $\{A, B^{(1)}, \dots, B^{(m)}\}$ are $d \times d$ matrices, $\Delta t = 1/N_T$ and $t_k = kT/N_T$ for $k = 0, 1, \dots, N_T$.

Proposition 4.8. *For the d -dimensional SDE with multiplicative Gaussian noise(35), the estimate*

$$\|\tilde{X}(T) - X(T)\|_2 \lesssim \Delta t,$$

holds for the solution \tilde{X} of the approximate equation(36).

Proof. We show this estimate by comparing the solution \tilde{X} to the Milstein approximation \hat{X} :

$$\hat{X}(t_{k+1}) = \hat{X}(t_k) + A\hat{X}(t_k)\Delta t + \sum_{l=1}^m B^{(l)}\hat{X}(t_k)\Delta W_k^{(l)} + \sum_{l,j=1}^m B^{(l)}B^{(j)}\hat{X}(t_k)I_k(j,l), \quad \hat{X}_{t_0} = x_0. \quad (37)$$

Here $I_k(j,l)$ represents the Ito's integral

$$I_k(j,l) = \int_{t_k}^{t_{k+1}} (W_s^{(j)} - W_{t_k}^{(j)})dW_s^{(l)}.$$

Using Ito's formula, it is clear that

$$I_k(l,j) + I_k(j,l) = \Delta W_k^{(l)} \Delta W_k^{(j)} \quad I_k(l,l) = \frac{1}{2}((\Delta W_k^{(l)})^2 - \Delta t).$$

In the $(k+1)$ -th iteration of (36), that is obtaining $\tilde{X}(t_{k+1})$ from $\tilde{X}(t_k)$, we know

$$\tilde{X}(t_{k+1}) = \exp(\tilde{A}_k \Delta t) \tilde{X}(t_k).$$

By the definition of the matrix exponential,

$$\exp(\tilde{A}_k \Delta t) = I + \tilde{A}_k \Delta t + \frac{1}{2} \sum_{l=1}^m \sum_{j=1}^m B^{(l)} B^{(j)} \Delta W_k^{(l)} \Delta W_k^{(j)} + \mathcal{O}(\Delta t \Delta W).$$

Comparing to the Milstein approximation \hat{X} in (37), we have,

$$\begin{aligned} \hat{X}(t_{k+1}) - \tilde{X}(t_{k+1}) &= \hat{X}(t_k) - \tilde{X}(t_k) + A(\hat{X}(t_k) - \tilde{X}(t_k)) \Delta t + \sum_{l=1}^m B^{(l)} (\hat{X}(t_k) - \tilde{X}(t_k)) \Delta W_k^{(l)} \\ &+ \frac{1}{2} \sum_{l=1}^m (B^{(l)})^2 (\hat{X}(t_k) - \tilde{X}(t_k)) ((\Delta W_k^{(l)})^2 - \Delta t) + \frac{1}{2} \sum_{\substack{l,j=1 \\ l \neq j}}^m B^{(l)} B^{(j)} (\hat{X}(t_k) - \tilde{X}(t_k)) I_k(j, l) \\ &+ \frac{1}{2} \sum_{\substack{l,j=1 \\ l \neq j}}^m B^{(l)} B^{(j)} \tilde{X}(t_k) (I_k(j, l) - \Delta W_k^{(l)} \Delta W_k^{(j)}) + \mathcal{O}(\Delta t \Delta W). \end{aligned} \quad (38)$$

It is clear that

$$\|A(\hat{X}(t_k) - \tilde{X}(t_k))\| \leq \|A\| \|\hat{X}(t_k) - \tilde{X}(t_k)\|, \quad \|B^{(l)}(\hat{X}(t_k) - \tilde{X}(t_k))\| \leq \|B^{(l)}\| \|\hat{X}(t_k) - \tilde{X}(t_k)\|.$$

We will next show that $\mathbb{E}\|\tilde{X}(t_k)\|^2$ and $\mathbb{E}\|\tilde{X}(t_k)\|$ is bounded for all k . The boundedness of $\mathbb{E}\|\tilde{X}(t_k)\|$ follows from $\mathbb{E}\|\tilde{X}(t_k)\|^2$ by Hölder's inequalities. A direct computation gives

$$\begin{aligned} \mathbb{E}\|\tilde{X}(t_k)\|^2 &= \mathbb{E}\|\exp(\tilde{A}_{k-1} \Delta t) \exp(\tilde{A}_{k-2} \Delta t) \cdots \exp(\tilde{A}_0 \Delta t) \tilde{X}(0)\|^2 \\ &\leq \mathbb{E}\left(\exp(2\|\tilde{A}_{k-1}\| \Delta t) \exp(2\|\tilde{A}_{k-2}\| \Delta t) \cdots \exp(2\|\tilde{A}_0\| \Delta t) \|\tilde{X}(0)\|^2\right) \\ &= \mathbb{E}\left(\|\tilde{X}(0)\|^2 \exp\left(2 \sum_{\tau=0}^{k-1} \|\tilde{A}_\tau\| \Delta t\right)\right) \end{aligned}$$

By the definition of \tilde{A}_k and the fact that $\Delta W_k^{(l)}$ are independent with each other, we have for every k ,

$$\mathbb{E}\|\tilde{X}(t_k)\|^2 \leq \|x_0\|^2 \exp\left[2(\|A\| + \frac{1}{2} \sum_{l=1}^m \|B^{(l)}\|^2) T\right] \prod_{\tau=0}^{N_T-1} \prod_{l=1}^m \mathbb{E}\left[\exp(2\|B^{(l)}\| |\Delta W_k^{(l)}|)\right] < \infty. \quad (39)$$

Squaring both sides and taking expectation of (38) gives

$$\begin{aligned} \mathbb{E}\|\hat{X}(t_{k+1}) - \tilde{X}(t_{k+1})\|^2 &= \mathbb{E}\left[(\hat{X}(t_{k+1}) - \tilde{X}(t_{k+1}))^\dagger (\hat{X}(t_{k+1}) - \tilde{X}(t_{k+1}))\right] \\ &= \mathbb{E}\|\hat{X}(t_k) - \tilde{X}(t_k)\|^2 + \mathbb{E}\|A(\hat{X}(t_k) - \tilde{X}(t_k))\|^2 \Delta t^2 + \sum_{l=1}^m \mathbb{E}\|B^{(l)}(\hat{X}(t_k) - \tilde{X}(t_k))\|^2 \Delta t \\ &+ \frac{1}{4} \mathbb{E}\left\|\sum_{l=1}^m (B^{(l)})^2 (\hat{X}(t_k) - \tilde{X}(t_k)) ((\Delta W_k^{(l)})^2 - \Delta t)\right\|^2 + \frac{1}{4} \mathbb{E}\left\|\sum_{\substack{l,j=1 \\ l \neq j}}^m B^{(l)} B^{(j)} (\hat{X}(t_k) - \tilde{X}(t_k)) I_k(j, l)\right\|^2 \\ &+ \frac{1}{4} \mathbb{E}\left\|\sum_{\substack{l,j=1 \\ l \neq j}}^m B^{(l)} B^{(j)} \tilde{X}(t_k) (I_k(j, l) - \Delta W_k^{(l)} \Delta W_k^{(j)})\right\|^2 + \mathbb{E}\left((\hat{X}(t_k) - \tilde{X}(t_k))^\dagger A(\hat{X}(t_k) - \tilde{X}(t_k)) \Delta t\right) \\ &- \frac{1}{4} \mathbb{E}\left(\sum_{\substack{l,j=1 \\ l \neq j}}^m (R_k^{(l,j)} + (R_k^{(l,j)})^\dagger) (I_k(j, l))^2\right) + \mathcal{O}(\Delta t^3). \end{aligned}$$

Here, we denote

$$R_k^{(l,j)} \triangleq (\widehat{X}(t_k) - \widetilde{X}(t_k))^\dagger (B^{(j)} B^{(l)})^\dagger B^{(l)} B^{(j)} \widetilde{X}(t_k).$$

and use the fact that

$$\mathbb{E}(I_k(j_1, l_1) I_k(j_2, l_2)) = \frac{1}{2} \delta_{j_1 j_2} \delta_{l_1 l_2} (\Delta t)^2, \quad \mathbb{E}(I_k(j, l) \Delta W_k^{(\tau)}) = 0.$$

By the fact that $\widehat{X}(t_k) - \widetilde{X}(t_k)$ is independent of $\Delta W_k^{(l)}$ and $I_k(j, l)$, we obtain

$$\begin{aligned} \mathbb{E} \left(\sum_{l=1}^m (B^{(l)})^2 (\widehat{X}(t_k) - \widetilde{X}(t_k)) ((\Delta W_k^{(l)})^2 - \Delta t) \right)^2 &= \sum_{l=1}^m \mathbb{E} \left((B^{(l)})^2 (\widehat{X}(t_k) - \widetilde{X}(t_k)) \right)^2 \mathbb{E} \left((\Delta W_k^{(l)})^2 - \Delta t \right)^2 \\ &\leq \tilde{C}_1 \mathbb{E} \|\widehat{X}(t_k) - \widetilde{X}(t_k)\|^2 \Delta t^2, \end{aligned}$$

and

$$\begin{aligned} \mathbb{E} \left(\sum_{\substack{l,j=1 \\ l \neq j}}^m B^{(l)} B^{(j)} (\widehat{X}(t_k) - \widetilde{X}(t_k)) I_k(j, l) \right)^2 &= \sum_{\substack{l,j=1 \\ l \neq j}}^m \mathbb{E} \|B^{(l)} B^{(j)} (\widehat{X}(t_k) - \widetilde{X}(t_k))\|^2 \mathbb{E}(I_k(j, l))^2 \\ &\leq \tilde{C}_2 \mathbb{E} \|\widehat{X}(t_k) - \widetilde{X}(t_k)\|^2 \Delta t^2. \end{aligned}$$

$$\begin{aligned} -\frac{1}{4} \mathbb{E} \left(\sum_{\substack{l,j=1 \\ l \neq j}}^m (R_k^{(l,j)} + (R_k^{(l,j)})^\dagger) (I_k(j, l))^2 \right) &\leq \frac{1}{4} \sum_{\substack{l,j=1 \\ l \neq j}}^m \mathbb{E} |R_k^{(l,j)} + (R_k^{(l,j)})^\dagger| \mathbb{E}(I_k(j, l))^2 \\ &\leq \tilde{C}_3 \sqrt{\mathbb{E} \|\widehat{X}(t_k) - \widetilde{X}(t_k)\|^2} \Delta t^2. \end{aligned}$$

Let $\epsilon_k = \mathbb{E}(\widehat{X}(t_k) - \widetilde{X}(t_k))^2$, then we know

$$\epsilon_{k+1}^2 \leq \epsilon_k^2 + C_1 \epsilon_k^2 \Delta t + C_2 \epsilon_k^2 \Delta t^2 + C_3 \epsilon_k \Delta t^2 + C_4 \Delta t^2 + C_5 \Delta t^3.$$

Here $\tilde{C}_1, \tilde{C}_2, \tilde{C}_3, C_1, C_2, C_3, C_4$ and C_5 are positive constants independent of Δt and k .

We will prove by induction that $\epsilon_k^2 = \mathcal{O}(\Delta t^2)$. Consider an auxiliary equation

$$\eta_{k+1}^2 = \eta_k^2 + C_1 \eta_k^2 \Delta t + C_2 \eta_k^2 \Delta t^2 + C_3 \eta_k \Delta t^2 + C_4 \Delta t^2 + C_5 \Delta t^3. \quad (40)$$

It is clear that $\epsilon_k \leq \eta_k$ and $\eta_k^2 = \mathcal{O}(\Delta t^2)$ implies $\epsilon_k^2 = \mathcal{O}(\Delta t^2)$. For every integer $1 \leq m \leq N_T$, assume for $k = 0, 1, \dots, m-1$, $\eta_k^2 = \mathcal{O}(\Delta t^2)$, we will prove $\eta_m^2 = \mathcal{O}(\Delta t^2)$. As η_k^2 is an increasing sequence, for a large enough constant $c > 0$, there exists $k_0 < m-1$ that $\eta_{k_0}^2 \leq c \Delta t^2$ and $\eta_{k_0+1}^2 \geq c \Delta t^2$. For $k_0 < k \leq m-1$,

$$\eta_{k+1}^2 \leq \eta_k^2 \left(\frac{C_4}{c} + 1 + (C_1 + \frac{C_3}{\sqrt{c}} + \frac{C_5}{c}) \Delta t + C_2 \Delta t^2 \right).$$

Then, by the fact that $\eta_{k_0}^2 = \mathcal{O}(\Delta t^2)$, one knows

$$\eta_m^2 \leq (\eta_{k_0}^2 + \tilde{C}_4 \Delta t^2 + \tilde{C}_5 \Delta t^3) \left(\frac{C_4}{c} + 1 + (C_1 + \frac{C_3}{\sqrt{c}} + \frac{C_5}{c}) \Delta t + C_2 \Delta t^2 \right)^m \leq C \Delta t^2.$$

Here, constants \tilde{C}_4, \tilde{C}_5 and C are irrelevant with m and Δt . We have proven that

$$\mathbb{E}(\widehat{X}(T) - \widetilde{X}(T))^2 = \mathcal{O}(\Delta t^2).$$

With the order 1-strong convergence of the Milstein method under the mean square norm (see, for example, [31, Theorem 10.3.5]), we conclude the approximate equation (36) strongly converges to the solution of the SDE (35) with at least order 1. \square

5 Summary

We proposed quantum algorithms for linear stochastic differential equations (SDEs) with both Gaussian noise and α -stable Lévy noise. The algorithms are based on solving approximate equations to the corresponding SDEs by the Schrödingerisation method. Compared to the Milstein scheme, the gates complexity of our algorithms exhibits a polylogarithmic dependence on both the dimensions and the number of samples, which demonstrates the quantum advantage over their classical counterparts in scenarios involving high dimensions and large sample sizes. We also obtained the convergence rate of the algorithms for SDEs with Gaussian noise in the mean square norm.

Our algorithms were applied to several examples, including Ornstein-Uhlenbeck processes, geometric Brownian motions and Lévy flights. It can be extended to general linear SDEs and reducible SDEs. It is also well-positioned for applications in areas such as Monte Carlo simulations, stochastic partial differential equations, and backward SDEs.

Acknowledgements

SJ and NL were supported by NSFC grant No. 12341104, the Shanghai Jiao Tong University 2030 Initiative and the Fundamental Research Funds for the Central Universities. SJ was also partially supported by the NSFC grants No. 12031013. NL acknowledges funding from the Science and Technology Program of Shanghai, China (21JC1402900). NL is also supported by NSFC grants No.12471411, the Shanghai Jiao Tong University 2030 Initiative, and the Fundamental Research Funds for the Central Universities.

References

- [1] Scott Aaronson and Alex Arkhipov. The computational complexity of linear optics. *Theory of Computing*, 9(4):143–252, 2013.
- [2] Dong An, Di Fang, and Lin Lin. Time-dependent unbounded Hamiltonian simulation with vector norm scaling. *Quantum*, 5:459, 2021.
- [3] Dong An, Di Fang, and Lin Lin. Time-dependent Hamiltonian simulation of highly oscillatory dynamics and superconvergence for Schrödinger equation. *Quantum*, 6:690, 2022.
- [4] Dong An, Noah Linden, Jin-Peng Liu, Ashley Montanaro, Changpeng Shao, and Jiasu Wang. Quantum-accelerated multilevel Monte Carlo methods for stochastic differential equations in mathematical finance. *Quantum*, 5:481, 2021.
- [5] Weizhu Bao and Shi Jin. High-order i -stable centered difference schemes for viscous compressible flows. *Journal of Computational Mathematics*, 21(1):101–112, 2003.
- [6] Pierre Barthelemy, Jacopo Bertolotti, and Diederik S Wiersma. A Lévy flight for light. *Nature*, 453(7194):495–498, 2008.
- [7] Fischer Black and Myron Scholes. The pricing of options and corporate liabilities. *Journal of Political Economy*, 81(3):637–654, 1973.
- [8] Yu Cao, Shi Jin, and Nana Liu. Quantum simulation for time-dependent Hamiltonians – with applications to non-autonomous ordinary and partial differential equations. *arXiv:312.02817*, 2023.
- [9] Andrew M. Childs, Robin Kothari, and Rolando D. Somma. Quantum algorithm for systems of linear equations with exponentially improved dependence on precision. *SIAM Journal on Computing*, 46(6):1920–1950, 2017.
- [10] Alvaro Corral. Universal earthquake-occurrence jumps, correlations with time, and anomalous diffusion. *Physical Review Letters*, 97(17):178501, 2006.

- [11] Valentin De Bortoli, James Thornton, Jeremy Heng, and Arnaud Doucet. Diffusion schrödinger bridge with applications to score-based generative modeling. In M. Ranzato, A. Beygelzimer, Y. Dauphin, P.S. Liang, and J. Wortman Vaughan, editors, *Advances in Neural Information Processing Systems*, volume 34, pages 17695–17709. Curran Associates, Inc., 2021.
- [12] Zhiyan Ding, Xiantao Li, and Lin Lin. Simulating open quantum systems using Hamiltonian simulations. *PRX Quantum*, 5(2):020332, 2024.
- [13] Tim Dockhorn, Arash Vahdat, and Karsten Kreis. Score-based generative modeling with critically-damped langevin diffusion. In *International Conference on Learning Representations*, 2022.
- [14] Crispin Gardiner. *Stochastic Methods*, volume 4. Springer Berlin, 2009.
- [15] Rémi Goerlich, Minghao Li, Samuel Albert, Giovanni Manfredi, Paul-Antoine Hervieux, and Cyriaque Genet. Noise and ergodic properties of Brownian motion in an optical tweezer: Looking at regime crossovers in an Ornstein-Uhlenbeck process. *Physical Review E*, 103:032132, 2021.
- [16] Javier Gonzalez-Conde, Ángel Rodríguez-Rozas, Enrique Solano, and Mikel Sanz. Efficient Hamiltonian simulation for solving option price dynamics. *Physical Review Research*, 5:043220, 2023.
- [17] Lov K. Grover. A fast quantum mechanical algorithm for database search. In *Proceedings of the Twenty-Eighth Annual ACM Symposium on Theory of Computing*, STOC '96, page 212–219, New York, NY, USA, 1996. Association for Computing Machinery.
- [18] Aram W. Harrow, Avinatan Hassidim, and Seth Lloyd. Quantum algorithm for linear systems of equations. *Physical Review Letters*, 103:150502, 2009.
- [19] Junpeng Hu, Shi Jin, Nana Liu, and Lei Zhang. Quantum circuits for partial differential equations via Schrödingerisation. *arXiv:2403.10032*, 2024.
- [20] Junpeng Hu, Shi Jin, and Lei Zhang. Quantum algorithms for multiscale partial differential equations. *Multiscale Modeling & Simulation*, 22(3):1030–1067, 2024.
- [21] Chin-Wei Huang, Jae Hyun Lim, and Aaron C Courville. A variational perspective on diffusion-based generative models and score matching. In M. Ranzato, A. Beygelzimer, Y. Dauphin, P.S. Liang, and J. Wortman Vaughan, editors, *Advances in Neural Information Processing Systems*, volume 34, pages 22863–22876. Curran Associates, Inc., 2021.
- [22] Gene Hunt. The relative importance of directional change, random walks, and stasis in the evolution of fossil lineages. *Proceedings of the National Academy of Sciences*, 104(47):18404–18408, 2007.
- [23] Shi Jin and Nana Liu. Analog quantum simulation of partial differential equations. *Quantum Science and Technology*, 9(3):035047, 2024.
- [24] Shi Jin, Nana Liu, and Chuwen Ma. On Schrödingerization based quantum algorithms for linear dynamical systems with inhomogeneous terms. *arXiv:2402.14696*, 2024.
- [25] Shi Jin, Nana Liu, and Chuwen Ma. Quantum simulation of Maxwell’s equations via schrödingerisation. *ESAIM: Mathematical Modelling and Numerical Analysis*, 58(5):1853–1879, 2024.
- [26] Shi Jin, Nana Liu, and Chuwen Ma. Schrödingerisation based computationally stable algorithms for ill-posed problems in partial differential equations. *arXiv:2403.19123*, 2024.
- [27] Shi Jin, Nana Liu, and Yue Yu. Quantum simulation of partial differential equations: Applications and detailed analysis. *Physical Review A*, 108:032603, 2023.
- [28] Shi Jin, Nana Liu, and Yue Yu. Quantum circuits for the heat equation with physical boundary conditions via Schrödingerisation. *arXiv:2407.15895*, 2024.
- [29] Shi Jin, Nana Liu, and Yue Yu. Quantum simulation of partial differential equations via Schrödingerization. *Physical Review Letters*, 133:230602, 2024.

- [30] Shi Jin, Nana Liu, and Yue Yu. Quantum simulation of the Fokker-Planck equation via Schrodingerization. *arXiv:2404.13585*, 2024.
- [31] Peter E Kloeden, Eckhard Platen, and Kloeden. *Numerical Solution of Stochastic Differential Equations*. Springer Berlin, Heidelberg, 1992.
- [32] Lingkai Kong, Jimeng Sun, and Chao Zhang. SDE-Net: Equipping deep neural networks with uncertainty estimates. In *Proceedings of the 37th International Conference on Machine Learning*, volume 119 of *Proceedings of Machine Learning Research*, pages 5405–5415. PMLR, 13–18 Jul 2020.
- [33] Lingkai Kong, Jimeng Sun, and Chao Zhang. SDE-net: Equipping deep neural networks with uncertainty estimates. In Hal Daumé III and Aarti Singh, editors, *Proceedings of the 37th International Conference on Machine Learning*, volume 119 of *Proceedings of Machine Learning Research*, pages 5405–5415. PMLR, 13–18 Jul 2020.
- [34] Kenji Kubo, Yuya O. Nakagawa, Suguru Endo, and Shota Nagayama. Variational quantum simulations of stochastic differential equations. *Physical Review A*, 103:052425, 2021.
- [35] Franziska Kühn and René L Schilling. Strong convergence of the Euler–Maruyama approximation for a class of Lévy-driven SDEs. *Stochastic Processes and their Applications*, 129(8):2654–2680, 2019.
- [36] Paul S. Lévy. Théorie de l’addition des variables aléatoires. *The Mathematical Gazette*, 39:344, 1955.
- [37] Guang Hao Low and Isaac L Chuang. Optimal Hamiltonian simulation by quantum signal processing. *Physical Review Letters*, 118(1):010501, 2017.
- [38] Ashley Montanaro. Quantum speedup of Monte Carlo methods. *Proceedings of the Royal Society A: Mathematical, Physical and Engineering Sciences*, 471(2181):20150301, 2015.
- [39] Yunseong Nam, Yuan Su, and Dmitri Maslov. Approximate quantum Fourier transform with $\mathcal{O}(n \log(n))$ t gates. *NPJ Quantum Information*, 6(1):26, 2020.
- [40] Román Orús, Samuel Mugel, and Enrique Lizaso. Quantum computing for finance: Overview and prospects. *Reviews in Physics*, 4:100028, 2019.
- [41] Peter W. Shor. Polynomial-time algorithms for prime factorization and discrete logarithms on a quantum computer. *SIAM Journal on Computing*, 26(5):1484–1509, 1997.
- [42] Yang Song, Jascha Sohl-Dickstein, Diederik P Kingma, Abhishek Kumar, Stefano Ermon, and Ben Poole. Score-based generative modeling through stochastic differential equations. In *International Conference on Learning Representations*, 2021.
- [43] G.M Viswanathan, V Afanasyev, Sergey V Buldyrev, Shlomo Havlin, M.G.E da Luz, E.P Raposo, and H.Eugene Stanley. Lévy flights in random searches. *Physica A: Statistical Mechanics and its Applications*, 282(1):1–12, 2000.
- [44] Jacob Watkins, Nathan Wiebe, Alessandro Roggero, and Dean Lee. Time dependent Hamiltonian simulation using discrete clock constructions. *arXiv:2203.11353*, 2024.
- [45] Pan Zhou, Jiashi Feng, Chao Ma, Caiming Xiong, Steven Chu Hong Hoi, and Weinan E. Towards theoretically understanding why sgd generalizes better than Adam in deep learning. In H. Larochelle, M. Ranzato, R. Hadsell, M.F. Balcan, and H. Lin, editors, *Advances in Neural Information Processing Systems*, pages 21285–21296. Curran Associates, Inc., 2020.